A novel self-nanoemulsifying drug delivery system for curcumin used in the treatment of wound healing and inflammation

Niyaz Ahmad[1,2] · Rizwan Ahmad[3] · Ali Al-Qudaihi[1] · Salman Edrees Alaseel[1] · Ibrahim Zuhair Fita[1] · Mohammed Saifuddin Khalid[4] · Faheem Hyder Pottoo[4] · Srinivasa Rao Bolla[5]

Abstract

The main objective of this study was to develop and evaluate self-nanoemulsifying drug delivery system (SNEDDS) of curcumin (Cur) to enhance their solubility as well as improve skin permeation; and evaluate wound healing potential of Cur via SNEDDS in comparison with standards pure eucalyptus oil-SNEDDS (Euc-SNEDDS), pure curcumin suspension (Cur-S), and standard fusidic acid followed by their anti-inflammatory action. Curcumin loaded different SNEDDS formulations were formulated through aqueous phase titration method and the zones of SNEDDS were recognized by the construction of phase diagrams. Eucalyptus oil, Tween 80 (surfactant), and Transcutol HP (co-surfactant) were selected on the basis of their solubility and highest nanoemulsion region. Characterization of thermodynamic stability for Cur-loaded SNEDDS was evaluated by its globule size, zeta potential, polydispersity index, viscosity, % transmittance, refractive index, and surface morphology. Cur-SNEDDS (Cur-SN4) was optimized and selected on the basis of their excellent physicochemical parameters for in vivo activity. The particle size (59.56 ± 0.94 nm), % transmittance ($99.08 \pm 0.07\%$), and PDI (0.207 ± 0.011 were observed for optimized Cur-SNEDDS. TEM and SEM showed their smooth and spherical shape of the morphological characterization with zeta potential (-21.41 ± 0.89), refractive index (1.341 ± 0.06), and viscosity (11.64 ± 1.26 cp) for optimized Cur-SNEDDS. Finally, optimized Cur-SNEDDS was used to enhance skin permeation with improvement in the solubility of Cur. However, optimized Cur-SNEDDS showed significant wound healing activity as compared with pure eucalyptus oil and Cur-S on topical application. Optimized Cur-SNEDDS showed healing of wound as compared to standard fusidic acid. Optimized Cur-SNEDDS exhibited no signs of inflammatory cells on the histopathological studies of treated rats which were recommended the safety and non-toxicity of Cur-SNEDDS. Newly developed Cur-SNEDDS could be successfully used to enhance Cur-solubility and skin permeation, as well as suggested a potential role of Cur-SNEDDS for better improvement of wound healing activity followed by anti-inflammatory action of Cur via topical application.

Keywords Curcumin · SNEDDS · Enhancement of solubility · Release and skin permeation study · Wound healing with anti-inflammatory action · Transdermal delivery

✉ Niyaz Ahmad
nahussain@iau.edu.sa; niyazpharma@gmail.com

1 Department of Pharmaceutics, College of Clinical Pharmacy, Imam Abdulrahman Bin Faisal University, Dammam, Kingdom of Saudi Arabia

2 Department of Pharmaceutical Chemistry, College of Clinical Pharmacy, Imam Abdulrahman Bin Faisal University, Dammam, Kingdom of Saudi Arabia

3 Department of Natural Products and Alternative Medicine, College of Clinical Pharmacy, Imam Abdulrahman Bin Faisal University, Dammam, Kingdom of Saudi Arabia

4 Department of Pharmacology, College of Clinical Pharmacy, Imam Abdulrahman Bin Faisal University, Dammam, Kingdom of Saudi Arabia

5 Department of Anatomy, College of Medicine, Imam Abdulrahman Bin Faisal University, Dammam, Kingdom of Saudi Arabia

Introduction

Skin generally injured physically, which causes the breaking or opening of skin is known as wounds (Singh et al. 2006; Pathan et al. 2019). Repairing of wounds is one of the most complicated physiologic processes. Different types of cells contribute to the healing of wounds (i.e., tightly regulated over time). The breakdown of this complicated path might be responsible for failure of wound healing, which causes non-healing wounds. Repairing of wounds involves different steps such as inflammation and generation of fresh tissues after that transformation of freshly formed tissue. All these mentioned stages are completed on intensely different timescales, up to minutes (i.e., first clotting followed by coagulation) to numerous months or many years (Gould et al. 2015; Boateng and Catanzano 2015). Pressure ulcers, arterial insufficiency, diabetic foot ulcers, and venous leg ulcers are caused by chronic wounds. Chronic wounds can cause extreme morbidity and also mortality in older peoples, who are affected by vascular diseases and diabetes mellitus. In general, older people generally recover after surgery when they are seriously affected by chronic wounds. Chronic wounds affect intensely the quality of life and its therapy needs very high quality of care (Stejskalova and Almquist 2017; Saporito et al. 2017). However, wounds are treated by different drugs with parenteral or oral routes, but can cause serious side effects or are affected by the initial deactivation of the drug.

Nanotechnologies based on drug delivery systems have an excellent potential role for the improvement of the pharmacological effects and their pharmacokinetic profile of plant-based bioactive materials and drug molecules (Jaiswal et al. 2015; Shakeel et al. 2015; Odei-Addo et al. 2017; Thiruvengadam et al. 2018; Alam et al. 2018; Ahmad et al. 2017a, b). Curcumin exhibits antioxidant activity which can play a great role in the treatment of wounds (Fitzmaurice et al. 2011; Thomas et al. 2017). Curcumin (a natural product) isolated from the rhizomes of *Curcuma longa* and is used orally and topically in wound healing. Curcumin (methoxyphenol derivative compound) shows antioxidant activity and excites the detoxification enzymes. Curcumin improves wound healing significantly when applied topically and also prevents oxidative damage (Gopinath et al. 2004). Curcumin improves the production of granulation in body tissue with more amount of cellular content and new vascularization, and also increases the process of re-epithelialization of wound (Sidhu et al. 1998). When a drug is poorly water soluble, it can be restricted to the superficial stratum corneum (SC) after topical delivery. We can use the lipophilic materials (e.g., curcumin) that can increase the amount of drug at the required place and the direct delivery of curcumin into the skin avoiding any systemic side effects. Thus, a new formulation is required which releases curcumin in a sustained or controlled form for its effective delivery. Nowadays, topical "self-nanoemulsifying drug delivery systems (SNEDDS)" and nanoemulsions have also been reported for the improvement of pharmacological effects of various therapeutic agents (El-Say et al. 2015; Badran et al. 2014; Ahmad et al. 2018a; Al-Rohaimi, 2015; Pratiwi et al. 2017). SNEDDS is a preconcentrate of nanoemulsions in which the drug is encapsulated in oil the phase in the presence of surfactant/co-surfactant which could form very fine nanosized droplets/nanoemulsions upon mild agitation with an aqueous media (Villar et al. 2012; Jain et al. 2015; Shakeel et al. 2015; Sharma et al. 2015). SNEDDS has numerous advantages in comparison to other colloidal drug carriers such as easy formulation, minimum cost preparation, and highest thermodynamic stability, followed by nanosized droplets (Villar et al. 2012; Shakeel et al. 2015; Sharma et al. 2015). As recently reported, the eucalyptus oil nanoemulsion formulations have a great potential for wound healing in rats (Alam et al. 2018). On the other hand, the wound-healing potential of curcumin with eucalyptus oil in the form of any nano-formulations such as SNEDDS had never been evaluated in the previous reported literature. The most important thing to be mentioned here is that for the in vivo activity, any active constituent of plant material, it is essential to take a standard or positive control to establish the potential effectiveness of that active phytoconstituent or plant material. It is also important that one more control should be taken as the positive control as a marketed preparation of the same particular active constituent of plant material or other available marketed preparation (as a reference) for the same activity. As an active phytoconstituent of plant, i.e., curcumin, is not available in the market for wound healing, we have used fusidic acid as a reference (i.e., positive control) to correlate the activity. Additionally, fusidic acid was used as an antibacterial agent in the treatment of wound healing. But there should be a bacterial infection is necessary. The bacterial infection is inhibited by fusidic acid in the treatment of wound healing to obtain its faster effects. Hence, we have chosen it as a positive control for the current study. Recently, clove and eucalyptus essential oil based nano-formulations have been reported potentially in the treatment of wound healing (Alam et al. 2017, 2018). Curcumin-loaded macroemulsions/normal emulsions were not evaluated in the current study; on the other side, topical SNEDDS formulations having smaller globule size in comparison to ordinary emulsions were evaluated. Therefore, SNEDDS has more in vivo benefits due to the improvement of absorption with therapeutic effects of essential oils and other phytoconstituents (Ahmad et al.

2017a, b; Ahmad et al. 2018a; Suqumar et al. 2014; Shakeel et al. 2015; Alam et al. 2018). Cur-loaded SNEDDS has more benefits over standard fusidic acid in that it does not produce adverse effects, has self-nanoemulsification efficiency, has thermodynamic stability, dose reduction is possible and it does not follow the first-pass metabolism. Hence, the aim of the present study was to develop suitable SNEDDS formulations of curcumin and to investigate its wound healing potential in rats in comparison with pure Cur-S (reference), eucalyptus oil (reference), marketed preparation of antibiotic fusidic acid (brand name: Fusidin: reference) with the use of wound excision rat model. Moreover, optimized Cur-SNEDDS was used to further evaluate the effect inflammatory study by skin drug delivery system with ex vivo skin permeation studies. Cur-SNEDDS was developed and optimized with the use of safe and nontoxic ingredients such as eucalyptus oil, Tween 80, Transcutol HP and water.

Materials and methods

Materials

Curcumin was obtained from (RxBiosciences, 18908 Bonanza way, Gaithersburg, MD20879, USA). Milli-Q water was purified using Milli-Q water purification system (ELGA, Made in UK). Transcutol HP, Tween 80, and other surfactants were purchased from Sigma Life Science, Sigma-Aldrich (Belgium). Methanol, ethanol, and acetonitrile (i.e., HPLC-grade having purity 99.9%) was procured from Sigma-Aldrich (Steinheim, Germany).

Excipients screening for the preparation of the final optimized nanoemulsion

Oil, surfactant and co-surfactant are used as excipients and their selection is based on the curcumin solubility and the formed stability of SNEDDS. Oleic acids, olive oil, almond oil, castor oil, eucalyptus oil, coconut oil, ethyl oleate, isostearyl isostearate and arachis oil were selected as oils. Based on biodegradability and easy accessibility, a very few number of oils were selected.

Tween 20, Labrasol®, Tween 80, Labrafil, PEG-400, PEG-200, propylene glycol, carbitol, Transcutol HP, and ethanol were selected as surfactants. Concisely; 1.0 ml oil or surfactant in microcentrifuge tube was added a maximum amount of Cur. After that, it was vortexed (72.0 h, 25.0 ± 1.0 °C) with the support of Remi CM-101 cyclomixer. The maximum amount of Cur was removed by centrifugation (Kubota Laboratory Centrifuge) of the mixtures for 10.0 min (3000 rpm), followed by 72.0 h. 10.0 µl of the supernatant was transferred to fresh tube and made up to a volume of 1.0 mL with ethanol. It was

filtered first with the help of a syringe filter (0.22 µm) followed by vortexing. We prepared a correct dilution for the UV absorbance at 427 nm to plot the calibration curve, followed by an unidentified amount of Cur dissolved in a definite amount of oil or surfactant (Parveen et al. 2011). We performed the excipient solubility study after that stability study of optimized Cur-SNEDDS.

Construction of pseudo-ternary phase diagrams

For preparation of the SNEDDS of Cur, pseudo-ternary phase diagrams were constructed by an aqueous phase titration method as reported by Ahmad et al. (2017b) and Shakeel et al. (2015). Briefly, Transcutol HP and Tween 80 were mixed in the mass ratios of 1:0, 1:1, 1:1, 2:1, 3:1, and 4:1. The total stock of the mixture of surfactant and co-surfactant (S_{mix}) was 20 g. Eucalyptus oil and a particular S_{mix} were then mixed at different mass ratios (i.e., 1:9 to 9:1). Pseudo-ternary phase diagrams were constructed by a spontaneous emulsification method. In this method, the mixture of eucalyptus oil and a certain S_{mix} was titrated by the slow addition of water and visual observations were recorded on the basis of clarity (Ahmad et al. 2017a, b, 2018a). The clear, transparent and easily flowable SNEDDS zones were plotted on each phase diagram with one axis representing water, the second eucalyptus oil and the third the S_{mix}.

Formulation development of curcumin

From pseudo-ternary phase diagrams, it was observed that the maximum SNEDDS zones were exposed by a 1:1 S_{mix} ratio; hence, a 1:1 mass ratio was chosen for the preparation of the SNEDDS of curcumin. From the phase diagram, different SNEDDSs with formulation codes of Cur-SN1 to Cur-SN9 were precisely selected. Almost the entire region of SNEDDS zones was taken into account. In formulations Cur-SN1–Cur-SN5, the concentration of the oil phase (eucalyptus oil) was kept constant at 5% w/w and the concentration of the S_{mix} varied from 10 to 50% w/w.

However, in formulations Cur-SN6–Cur-SN9, the concentration of the S_{mix} was kept constant at 40% w/w and the concentration of the oil phase varied from 10 to 25% w/w to cover the entire SNEDDS zones in the phase diagram. After selection of a blank SNEDDS from the phase diagram, 5% w/w of curcumin was incorporated in each SNEDDS by vortexing at 1000 rpm and 25 °C for about 5 min. The composition of the curcumin-loaded SNEDDS is shown in Table 1.

Thermodynamic stability and self-nanoemulsification tests

Thermodynamic stability tests on the developed Cur-loaded SNEDDS (Cur-SN1 to Cur-SN9) were performed to remove

Table 1 Formulation components of SNEDDS formulations of curcumin (Cur-SN1−Cur-SN9) prepared using eucalyptus oil, Tween 80, Transcutol HP, and water

Formulation composition (% w/w)						
Formulation code	Curcumin	Eucalyptus oil	Tween 80	Transcutol HP	Water	S_{mix} ratio
Cur-SN1	5	5	25	25	40	1:1
Cur-SN2	5	5	20	20	50	1:1
Cur-SN3	5	5	15	15	60	1:1
Cur-SN4	5	5	10	10	70	1:1
Cur-SN5	5	5	5	5	80	1:1
Cur-SN6	5	10	20	20	45	1:1
Cur-SN7	5	15	20	20	40	1:1
Cur-SN8	5	20	20	20	35	1:1
Cur-SN9	5	25	20	20	30	1:1

any unstable or metastable formulation. These tests were performed viz. centrifugation, heating, and cooling cycles and freeze–pump–thaw cycles. The detailed procedures of these tests are given by Ahmad et al. (2017a, b) and Shakeel et al. (2015). Phase separation or precipitation test was performed with acid buffer (0.10 N HCl), phosphate buffer (pH 7.40), and water to confirm the self-nanoemulsification. This test was performed through diluting 1.0 mg per mL of every Cur-loaded SNEDDS (Cur-SN1 to Cur-SN9) with water, 0.10 N HCl, and phosphate buffer (pH 7.40) in the dilution ratio of 1:500. Every formulation's self-nanoemulsification efficiency was evaluated through visual observation on the basis of grade systems: (Ahmad et al. 2017a, b, 2018b; Shakeel et al. 2015).

Grade A: rapid/spontaneously forming clear nanoemulsion.

Grade B: rapid/spontaneously forming bluish slightly less clear nanoemulsion.

Grade C: slowly forming turbid emulsion.

Grade D: dull, grayish slowly forming turbid emulsion.

Grade E: turbid emulsion with the presence of oil globules at the surface.

Physicochemical characterization of the Cur-SNEDDS

Developed curcumin loaded SNEDDS was characterized physicochemically to determine its polydispersity index (PDI), distribution of droplet size, zeta potential (ZP), refractive index (RI), viscosity, % transmittance (%T), and surface morphology by scanning electron microscopy (SEM) and transmission electron microscopy (TEM). Developed formulations (Cur-SN1 to Cur-SN9) were characterized first on the basis of ZP, PDI, and droplet size by the Malvern Particle Size Analyzer (Holtsville, NY, USA), followed by a previously reported method (Ahmad et al. 2018c). The viscosity of the prepared Cur-SNEDDSs (Cur-SN1 to Cur-SN9) was measured at 25 ± 0.5 °C as such before and after dilution by Brookfield viscometer R/S CPS Plus (Brookfield

Engineering Laboratories Inc., Middleboro, MA, USA) using spindle C 50–1 at 25 ± 0.5 °C temperature. The spindle no. 50 is used at a speed of 70 rpm at shear stress of 413 per min and wait time kept at 15 min. Finally, the shear rate produced as a parameter of viscosity was noted in terms of centipoises (Ahmad et al. 2018b). The Cur-SNEDDSs (Cur-SN1 to Cur-SN9) refractive indexes were determined with the help of Abbe type refractometer (Precision Testing Instruments Laboratory, Germany) (Ahmad et al. 2018b). Cur-SNEDDSs (Cur-SN1 to Cur-SN9) percentage transmission was examined spectrophotometrically at 427 nm as used by Ahmad et al. (2018b, 2019a). Optimized Cur-SNEDDSs (Cur-SN1 formulation) was also characterized by the surface morphology and droplet structure with the help of scanning electron microscopy (SEM) ((FEI, INSPECT S50, Check Republic) and transmission electron microscopy TEM (FEI, MORGAGNE.68, Check Republic). 100 kV was set to operate the electron microscopy at the time of SEM and TEM analysis. Characterization of the developed and optimized Cur-SNEDDSs (Cur-SN1 formulation) for the SEM and TEM method was done using a previously reported method Ahmad et al. (2018b, 2019a).

Differential scanning calorimetry (DSC)

DSC 214 Polyma (NETZSCH-Wittelsbacherstraße 42, 95100 Selb, Germany) known was carried out in order to confirm the complete solubilization as well as incorporation of the drug in the SNEDDS which is based on the DSC data analysis of Cur, Tween 80, Transcutol HP, eucalyptus oil, and optimized Cur-SNEDDS. In brief, the sample was kept in the pan (10.0 mg), whereas the empty pan was taken as reference. For the instrument, we selected a temperature range (40.0–400.0 °C) based on the temperature increase determined as 10°K/min with the help of nitrogen flow (maintained 60.0 ml/min) (Ahmad et al. 2018a, b). DSC 214 Polyma (NETZSCH-PROTEUS-70, Germany) software was used to obtain the value.

FT-IR with ATR

Functional groups of the compounds with their chemical structure and composition were characterized through FT-IR with ATR (NICOLET iS50 FT-IR; Thermo Fisher Scientific, 5225 Verona Road, Madison, WI 53711, USA). IR spectra of pure curcumin, Tween 80, eucalyptus oil, Transcutol HP, and curcumin self-nanoemulsifying drug delivery systems (Cur-SNEDDS) were determined by an attenuated total reflectance (ATR, wavenumber 4000–400 cm$^{-1)}$. Pure curcumin, Tween 80, eucalyptus oil, Transcutol HP, and curcumin self-nanoemulsifying drug delivery system (Cur-SNEDDS) were directly analyzed without any special preparation.

In vitro drug release

The in vitro release profile of the curcumin−suspension and optimized Cur-loaded SNEDDS was carried out with the help of dialysis sacs (MWCO 12,000 g/mole; Sigma-Aldrich). A cellulose membrane dialysis sac was filled with equivalent volume of Cur-loaded optimized-SNEDDS (Cur: 2.0 mg) and the experiment was performed with the help of dissolution apparatus 2 (Veego, Mumbai, India) having 500 mL of PBS (pH 7.4) at 37.0 °C ± 1.0 °C (Ahmad et al. 2018c; Sood et al. 2014). On the basis of already established time intervals, aliquots were taken out from the released medium and replaced with the phosphate buffer. The samples were examined in triplicate using the previously reported UHPLC–MS/MS method (Ahmad et al. 2017a, b).

Permeability skin study (ex vivo)

We followed Ahmad et al.'s method to perform the skin permeation study (Ahmad et al. 2018a, c).

In vivo study

For the in vivo pharmacodynamic and histopathological studies, a proper ethical approval was obtained from the Animal Ethical Committee, Imam Abdulrahman Bin Faisal University (Dammam, Saudi Arabia). All animal procedures were performed in accordance with the Guidelines for Care and Use of Laboratory Animals of "Imam Abdulrahman Bin Faisal University" and approved by the "Institutional Animal Care and Use Committee (IACUC)" with "Institutional Review Board (IRB Approval Number: IRB-UGS-2018-05-200)". Albino rats (weight; 180–200 g) were grouped (5–10 in each cage) and maintained in a natural light and dark cycle with free access to food and water (temperature 20.0–30.0 C; humidity 50.0–55.0%). All animals were kept under laboratory-prescribed conditions. Research activity was started during the light cycle in the waking condition using freely moving animals.

Histomorphological evaluation of tissues

Groups of healed tissues of rats were taken at the end of the experiment (after 24 days) to perform the histomorphological analysis in which formalin (10.0%), dehydrated alcohol with paraffin blocks were used. Xylene was used to deparaffinize tissues sections. Microtome was used to cut the selected diameter of the sections and stained by HE (hematoxylin–eosin) followed by analysis of light microscope. Inflammation was identified blindly in the healed areas, whereas infiltrations or their field of inflammatory cells were counted. Healed area of tissue was evaluated by inflammatory cell infiltration, epithelization, neovascularization, fibroblast proliferation, and collagen deposition. The reported modified scale is 0.0–5.0 for wound healing area [33,41].

Evaluation of wound healing area

Evaluation of wound healing area was performed in Group I: control group optimized SNEDDS without Cur loaded; Group II: pure eucalyptus oil (10 mg/kg body. wt.); Group II: pure Cur-5 mg/kg body. wt.); Group III: optimized Cur-SNEDDS (Cur-SNEDDS; 10 mg/kg body. wt.) and marketed preparation of antibiotic fusidic acid (brand name: Fusidin; 10 mg/kg body. wt. served as positive control). Wistar rats strain, female albino weight: 200.0–250.0 g) were taken for this research. Five groups (6 rats in each group; $6 \times 5 = 35$) were taken to perform this research study for the evaluation of wound healing area. Before making the wounds on the rats, we performed anesthesia with epilation. Excision of wound was performed on an approximately predetermined area (500 mm^2 maximum thickness) on the anterior-dorsal side of each female rat (Ahmad et al. 2018c; Shakeel et al. 2019). All the female rats received topically the test formulations once daily, in their respective groups, up to 24 days. The percentage of wound contractions and their healing time are the best parameters to analyze the wound healing. We determined the wound area on every 3rd day by keeping a butter paper and drawing the wound area. The percentage of wound contractions was calculated on the area by placing a graph sheet (Ahmad et al. 2018c; Shakeel et al. 2019). The total wound healing area and their closing area were determined.

Cur-SNEDDS treatment for inflammation

All the rat groups were further divided into two rats in each cage with their weights 200.0–250.0 g. Rats were allowed to take food and water freely at all times, maintaining 20.0–30.0 °C temperature, 50.0–55.0% humidity, and natural light and dark cycle. Finally, we quickly maintained the laboratory conditions to perform the experiments and wake up

cycle with freely moving rats. For each group, the rat's skin was previously depilated on the dorsal side; Cur-SNEDDS and Cur-S (one teaspoonful) were applied topically. Carrageenan injection (1% normal saline suspension; 100.0 µl) was given previously to develop inflammation at the right hind paw (Ahmad et al. 2018c; Moghaddam et al. 2018).

In the left hind paw, the same amount of non-pyrogenic normal saline solution was injected to serve as control. Paw thickness was evaluated for every 4.0 h through digital plethysmograph (UGO Basile, Italy) and also the percentage change of edema calculated. Each female rat serves as her own control. Paw thickness (control means saline-injected) was evaluated for each measurement. This one was compared with the inflamed paw for each female rat for evaluation at all sampling time points.

Statistical analysis

All outcomes will be evaluated and represented as mean ± SEM (standard error of mean). Student's *t* test was used for the unpaired observation calculation and their difference with the help of ANOVA, i.e., *p* value.

Result and discussion

### Excipients screening for the preparation of final optimized nanoemulsion

Curcumin solubility was determined in various oils (oleic acid, castor oil, olive oil, almond oil, eucalyptus oil, coconut oil, isostearyl isostearate, ethyl oleate, arachis oil) as displayed in Fig. 1. Finally, we selected four oils (eucalyptus oil, coconut oil, almond oil, olive oil) that showed the

maximum solubility. In Fig. 1, Tween 80 having the HLB value 15.00 shows maximum solubility and after that Transcutol HP (a medium chain fatty acid). Because of molecular weight, Tween 80 reduced the particle size when compared with other polymeric surfactants (Ghosh et al. 2013). Literature clearly reports that the HLB value of the surfactant lowers the interfacial energy, which leads to formation of a stable emulsion. The surfactant added in SNEDDS formulation, i.e., Tween 80, has HLB value of 15. Thus, HLB values and ternary plots obtained indicated the synergistic effect in reducing interfacial tension and the formation of stable nanoemulsion. On the other hand, Transcutol HP (with an HLB of 4.2) has several exceptional advantages over the traditional ones, including better stability, good emulsification efficiency (mainly with Tween 80), and less volatility (Nasr et al. 2016b; Monika and Saxena 2019). On the basis of these properties, Tween 80 and Transcutol HP were selected as surfactant and co-surfactants.

Additionally, oil and surfactant, and co-surfactant screening was based on particle size, PDI, and % transmittance to prepare a stable nanoformulation. Cur-SN4 formulation showed the lowest particle size and PDI (59.56 ± 0.94 and 0.207) as depicted in Table 4, which is based on the surfactants and oil, Tween 80, Transcutol HP, and eucalyptus oil followed by the final selection of combination. The selection of eucalyptus oil is defensible because of its renowned health benefits, i.e., wound healing, anti-inflammatory, antioxidant, healing bronchial asthma and vaginal infections as reported (Alam et al. 2018; Juergens et al. 2003; Silveira et al. 2013).

Tween 80 and Transcutol HP combination of surfactants and co-surfactants was thermodynamically stable with a good emulsification efficiency, minimum size droplet, higher in vitro drug release, and optimal drug diffusion. This combination was previously used by some other research

Fig. 1 Solubility of curcumin in different oils, surfactants, and co-surfactants
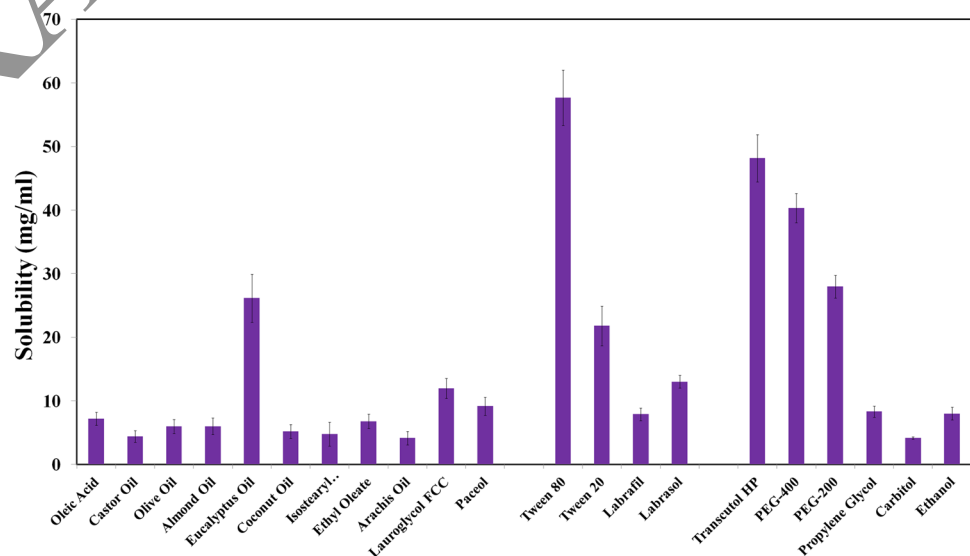
(Nipun and Islam 2014; Cirri et al. 2018; Khan et al. 2015; Nasr et al. 2016a), in which the co-surfactant produced the SNEDDS with reduced particle size, enhanced permeability, and improved bioavailability of drugs. They produced a very small zeta potential. Non-ionic surfactant will produce a very small zeta potential on the charge of the surface, followed by reducing the particle size of SNEDDS/NE (Nipun and Islam 2014; Cirri et al. 2018; Khan et al. 2015; Nasr et al. 2016a; McClements and Xiao 2012).

Construction of pseudo-ternary phase diagrams and formulation development

Eucalyptus oil, Tween 80, Transcutol HP, and water were taken to construct the pseudo-ternary phase diagrams for development of the Cur-SNEDDS. Figure 2 and Table 2 shows the results for this study. 1:0 S_{mix} ratios exhibited clearly the poor zones of the SNEDDS in Fig. 2a. 1:0 S_{mix} ratio showed the maximum amount of eucalyptus oil (oil phase) solubilized,
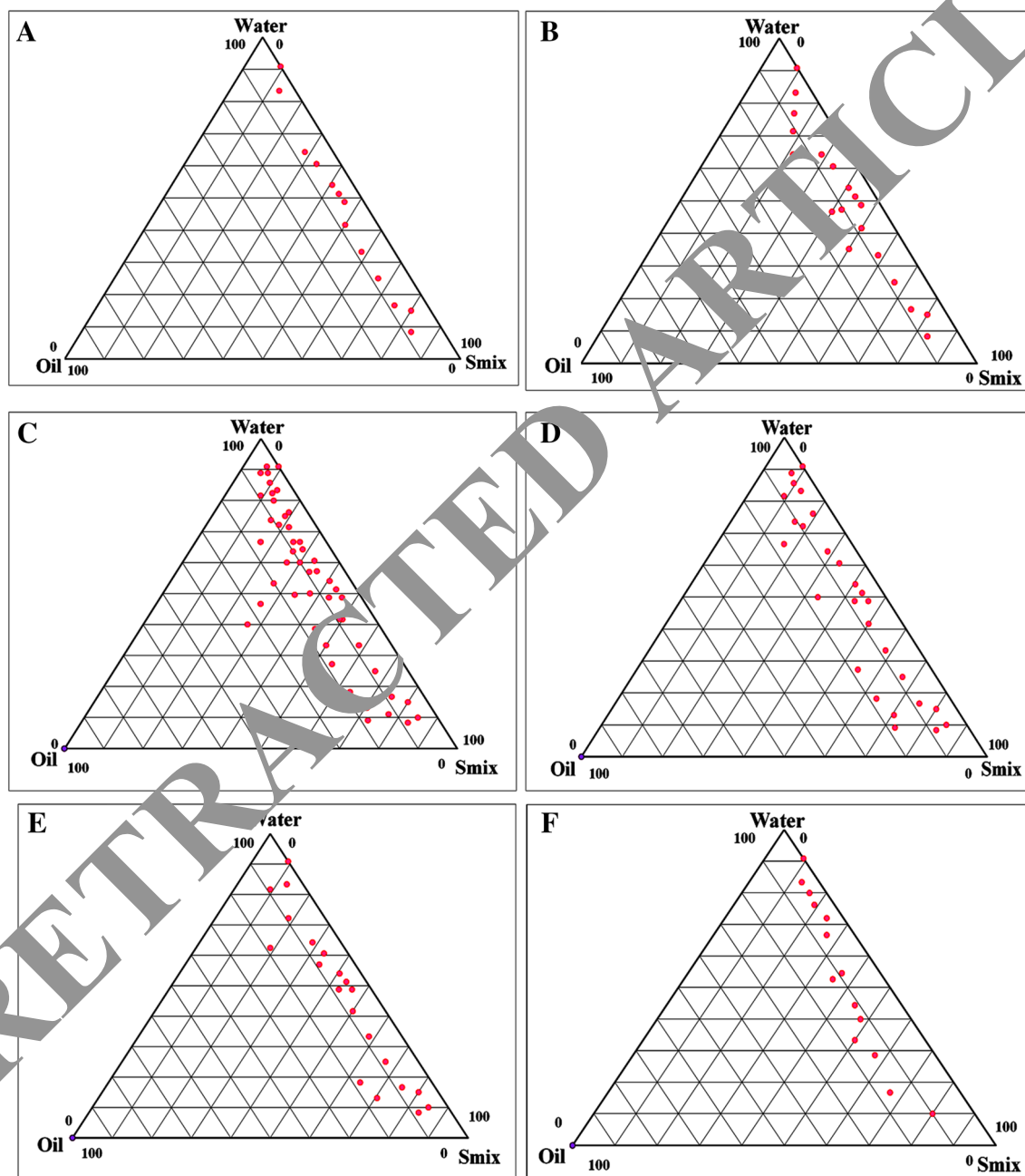

Fig. 2 Phase diagrams developed by the aqueous phase titration method for SNEDDS zones of curcumin (dotted area) for eucalyptus oil, Milli-Q-water, Tween 80 and Transcutol HP at S_{mix} ratios of **a** 1:0, **b** 1:2, **c** 1:1, **d** 2:1, **e** 3:1, and **f** 4:1

Table 2 Summary of observations made during the aqueous phase titration of SNEDDS

Figure	S_{mix} ratio	Surfactant	Co-surfactant	Nanoemulsion zones	Oil phase solubilized[a] (% w/w)	S_{mix} solubilized[b] (% w/w)
1A	1:0	Tween 80	Transcutol HP	Low	10	84
1B	1:2	Tween 80	Transcutol HP	Higher than 1A	15	58
1C	1:1	Tween 80	Transcutol HP	Highest	29	43
1D	2:1	Tween 80	Transcutol HP	Lower than 1C	23	54
1E	3:1	Tween 80	Transcutol HP	Lower than 1C and 1D	17	6
1F	4:1	Tween 80	Transcutol HP	Lower than 1C, 1D, and 1E	16	61

[a]The maximum amount of eucalyptus oil (oil phase) that was solubilized

[b]The maximum amount of the S_{mix} (Tween 80:Transcutol HP) phase that was solubilized with respect to the maximum amount of the oil phase

in which 10% w/w related to 84% w/w of the S_{mix}. For the 1:2 S_{mix} ratios, co-surfactant Transcutol HP amount enhanced with respect to the surfactant Tween 80, and SNEDDS zone areas were also increased in comparison to the 1:0 S_{mix} ratio (Fig. 2b). 1:2 S_{mix} ratio showed the maximum amount of eucalyptus oil (oil phase) solubilized in which 15% w/w of oil phase related to 58% w/w of the S_{mix} (Table 2) which was greater than that represented in Fig. 2a. The 1:1 S_{mix} ratio of surfactant and co-surfactant were shown to increase SNEDDS zones significantly as compared to previous S_{mix} ratios (Fig. 2c). The 1:1 S_{mix} ratio showed the maximum amount of eucalyptus oil (oil phase) solubilized in which 29% w/w of oil phase related to S_{mix} (43% w/w) (Table 2), though 2:1 S_{mix} ratio SNEDDS regions were decreased in comparison to 1:1 S_{mix} ratio (Fig. 2d). The 2:1 S_{mix} ratio showed the maximum amount of eucalyptus oil (oil phase) solubilized in which 23% w/w of oil phase related to S_{mix} (54% w/w) (Table 2). For the 3:1 S_{mix} ratio, Tween 80 concentration increased in relation with Transcutol HP, and SNEDDS zones were reduced in comparison to the 2:1 and 1:1 ratios (Fig. 2e). The 3:1 S_{mix} ratio showed the maximum amount of eucalyptus oil (oil phase) solubilized in which 17% w/w of oil phase related to S_{mix} (69% w/w) (Table 2). For the 4:1 S_{mix} ratio, Tween 80 concentration increased in relation with Transcutol HP, and SNEDDS zones were reduced in comparison to the 3:1, 2:1 and 1:1 ratios (Fig. 2f). The 4:1 S_{mix} ratio showed the maximum amount of eucalyptus oil (oil phase) solubilized in which 16% w/w of oil phase related to S_{mix} (61% w/w) (Table 2). The 1:1 S_{mix} ratio showed the maximum SNEDDS zones by the aqueous phase titration studies (Fig. 2c). Hence, various SNEDDS formulations of eucalyptus oil were chosen from Fig. 2c. The whole region of Fig. 2c was selected as SNEDDS zones. 5.0% w/w eucalyptus oil concentration was kept constant in the S_{mix} concentration, i.e., 10.0−50.0% w/w for the first five formulations (Cur-SN1–Cur-SN5). On the other hand for four formulations (Cur-SN6–Cur-SN9), the concentration of S_{mix} was fixed (i.e., 40% w/w) and the eucalyptus oil concentration was varied from 10 to 25% w/w so as to

take the complete SNEDDS zone, as Fig. 2c. We selected the placebo-SNEDDS and after that curcumin (5% w/w) was incorporated in every SNEDDS through vortexing at 1000 rpm and 25.0 °C for 5.0 min (Table 1).

Thermodynamic stability and self-nanoemulsification tests

A thermodynamic stability test was the main objective of this current study, in which any metastable/unstable SNEDDS were taken out as per the visual observations of phase titration studies. Therefore, different types of thermodynamic stability tests were performed on the various curcumin selected formulations which are shown in Table 3. It was observed that each prepared SNEDDSs passed various thermodynamic stability tests shown in the Table 3. These self-nanoemulsification efficiency tests were compulsory tests for topical emulsifying formulations of the prepared curcumin formulations (Cur-SN1 to Cur-SN9) (Ahmad et al. 2018a). Phase separation or drug precipitation was the main objective of this test which was performed by gentle agitation with water, 0.10 N HCl acid buffer, and phosphate buffer (pH:6.80), as shown in Table 3 (Ahmad et al. 2016a). All the Cur-loaded SNEDDSs passed this test with all these three agents in which all transparent Cur-loaded SNEDDSs passed the test with a grade of A. These were taken as the best Cur-loaded SNEDDSs formulations. Overall, these results indicated that curcumin was maintained in a solubilized form at the molecular state in developed SNEDDSs and the self-nanoemulsification behavior of all the formulations was independent of pH (Ahmad et al. 2016a, 2017a, b; Shakeel et al. 2015).

Physicochemical characterization of the Cur-SNEDDS

All the physicochemical examination results for Cur-SNEDDS (Cur-SN1 to Cur-SN9) are shown in Table 4. The

Table 3 Thermodynamic stability test for SNEDDS in the Milli-Q-water, 0.10 N hydrochloric acid and phosphate buffer (pH 6.80)

Formulation code	Grades* (for SNEDDS test)	Thermodynamic stability test		
		Centrifugation	Heating and cooling cycles	Freeze–pump–thaw cycles
Cur-SN1	A	√	√	√
Cur-SN2	A	√	√	√
Cur-SN3	A	√	√	√
Cur-SN4	A	√	√	√
Cur-SN5	A	√	√	√
Cur-SN6	A	√	√	√
Cur-SN7	A	√	√	√
Cur-SN8	A	√	√	√
Cur-SN9	A	√	√	√

√ and * = Passed all three above proposed tests for all nine formulations with grade A

most important parameter of characterization was optimized Cur-loaded SNEDDS globule size. It was found that the droplet size of the Cur-SNEDDS (Cur-SN1 to Cur-SN9) was from 9.01 to 133.89 nm, as in Table 4. 5.0% w/w eucalyptus oil (oil phase) concentration was fixed constant; on the other side, 10.0 to 25.0% w/w S_{mix} concentration was taken as 10.0 to 50.0% w/w (Cur-SN1 to Cur-SN5) in which Cur-SNEDDS droplet size was observed to be less than 60 nm. It means that it has been changed considerably. S_{mix} concentration was increased with slight decrease in the formulations droplet size (Table 4). But the S_{mix} concentration was kept constant and eucalyptus oil concentration was taken from 5.0 to 25.0% w/w (Cur-SN6–Cur-SN9), Cur-SNEDDS droplet size was found to alter significantly. When the concentration of eucalyptus oil increased, the droplet size of the mentioned formulations enhanced quickly in the Cur-SNEDDS (Table 4). On the basis of observed results, eucalyptus oil had a high impact droplet size of the Cur-SNEDDS, but S_{mix} concentration showed small impact on the droplet size of the Cur-SNEDDS. In general, the maximum droplet size was identified in Cur-SN9 formulation (133.89 ± 4.01 nm)

that could be possibly due to the maximum amount of eucalyptus oil presence (i.e., 25% w/w) in the Cur-SN9. But, the smallest droplet size of the Cur-SNEDDS (Cur-SN1) was identified as 9.01 ± 0.63 nm due to the smallest quantity of eucalyptus oil (i.e., 5% w/w) in Cur-SN1.

Measurement of the PDI is useful to evaluate the uniformity of the droplets in the developed SNEDDS. PDIs of the Cur-SNEDDS (Cur-SN1 to Cur-SN9) were recorded as 0.106–0.396 as shown in Table 4. The least PDI was observed in the Cur-SNEDDS (Cur-SN1) (0.106), indicating higher uniformity of the droplet size distribution as compared to other Cur-SNEDDS. However, the highest PDI value was observed in the Cur-SNEDDS (Cur-SN9) (0.396). Overall, the PDIs were less than 0.40 in all formulations, indicating good uniformity of the droplet size distribution in all formulations. Here, the most important observation was the particle size Cur-SNEDDS (Cur-SN1 to Cur-SN9) recorded as 9.01 ± 0.63 nm to 133.89 ± 4.01 nm, as shown in Table 4. All the Cur-SNEDDS (Cur-SN1 to Cur-SN9) formulation showed greater increment in the particle size in comparison to PDI, which showed less variations and

Table 4 Optimization of best Cur-SNEDDS on the basis of different parameters

Formulation code	Optimization parameters					
	Droplet size ± SD (nm)	PDI	Zeta potential (mV)	Viscosity ± SD (cp)	Refractive index (RI)	% Transmittance ± SD
Cur-SN1	9.01 ± 0.63	0.106	− 29.97	11.98 ± 0.94	1.416 ± 0.04	93.16 ± 0.04
Cur-SN2	21.38 ± 0.68	0.154	− 28.84	12.78 ± 1.05	1.420 ± 0.05	95.46 ± 0.04
Cur-SN3	33.44 ± 0.36	0.198	− 27.45	13.54 ± 1.16	1.421 ± 0.05	97.41 ± 0.05
Cur-SN4	59.56 ± 0.94	0.207	− 21.41	11.64 ± 1.26	1.441 ± 0.06	99.08 ± 0.07
Cur-SN5	18.46 ± 0.56	0.158	− 26.42	11.56 ± 0.96	1.411 ± 0.04	96.75 ± 0.06
Cur-SN6	89.47 ± 1.64	0.285	− 18.01	21.49 ± 1.54	1.456 ± 0.07	92.46 ± 0.08
Cur-SN7	124.37 ± 2.09	0.298	− 16.71	31.75 ± 2.46	1.461 ± 0.08	94.57 ± 0.07
Cur-SN8	111.36 ± 3.48	0.349	− 15.65	38.45 ± 2.79	1.467 ± 0.08	96.47 ± 0.08
Cur-SN9	133.89 ± 4.01	0.396	− 13.55	47.64 ± 3.11	1.489 ± 0.09	95.42 ± 0.07

greater uniformity of the droplet size distribution among all the formulations.

Determination of the zeta potential is also a most important parameters for the characterization of the total surface charge and stability of the optimized Cur-SNEDDS. For the optimized Cur-SNEDDS formulations (Cur-SN1 to Cur-SN9) of the zeta potential values were found as − 29.97 to − 13.55 mV (Table 4). The smallest zeta potential value was identified in the Cur-SNEDDS, i.e., Cur-SN1 (− 29.97 mV). But the highest value of the zeta potential was found in the Cur-SNEDDS Cur-SN9 (− 13.55 mV). The −ve zeta potential values in each Cur-SNEDDS may be due to the presence of −ve charged fatty acid esters in eucalyptus oil (Alam et al. 2018). Zeta potential values of optimized Cur-SNEDDS formulations observed experimentally in the magnitude of ± 25 mV showed the Cur-SNEDDS stable formulation (Alam et al. 2018).

Viscosity determination is also essential to assess the flow behavior of the prepared SNEDDS. The viscosity of all developed formulations (Cur-SN1 to Cur-SN9) was observed from 11.98 to 47.64 cp (Table 4). All the viscosity values were related with all compositions of formulation and their globule sizes. When the 5.0% w/w eucalyptus oil concentration was kept constant and the concentration of S_{mix} was changed from 10.0 to 50.0% w/w (Cur-SN1–Cur-SN5), it was found that Cur-SNEDDS viscosity was altered slightly. The developed formulation (Cur-SN1 to Cur-SN5) viscosity was observed to reduce slightly in comparison to the concentration of S_{mix} (Table 4). If the quantity of the S_{mix} was kept constant and eucalyptus oil quantity was taken as 10.0–25.0% w/w (Cur-SN6–Cur-SN9), it was observed that the Cur-SNEDDS viscosity changed radically. From Cur-SN6 to Cur-SN9, viscosity was observed to enhance significantly with enhancing eucalyptus oil concentration (Table 4). Furthermore, all Cur-SNEDDs viscosity was also observed to decrease with a reduction in the droplet size of the developed formulation. Therefore, it showed that S_{mix} had a small effect on viscosity of the Cur-SNEDDS. On the other hand, eucalyptus oil and the droplet size had a better effect on Cur-SNEDDS viscosity. Finally, the smallest and maximum viscosities were also noted in the Cur-SNEDDS Cur-SN1 (11.98 ± 0.94 cp) and (Cur-SN9) (47.64 ± 3.11cp), respectively. This is the most important point for the viscosity having smaller values for all developed Cur-SNEDDS (Cur-SN1–Cur-SN9) formulations were responsible for the free flowing behavior of all developed formulations.

Refractive index (RI) determination is also useful to determine the transparent behavior and nanoemulsion type. Cur-SNEDDS (Cur-SN1–Cur-SN9) refractive indexes (RIs) were found in the optimized range, i.e., 1.416–1.489 (Table 4). The RIs maximum value was noted in the Cur-SNEDDS Cur-SN9 (1.489 ± 0.09). On the other hand, RIs smallest value was noted in the Cur-SNEDDS (Cur-SN1)

(1.416 ± 0.04). All the values of refractive indexes for the optimized formulations were very near the refractive index value of water (1.441), therefore it is an indication of the transparent nature and oil-in-water (o/w) type behavior of all Cur-SNEDDS.

Optimized Cur-SNEDDS formulations (Cur-SN1 to Cur-SN9) of the zeta potential values were found to be − 29.97 to − 13.55 mV, but in the case of Cur-SNEDDS (Cur-SN1–Cur-SN9) the refractive indexes (RIs) were found in the optimized range, i.e., 1.416–1.489 (Table 4). The German physicist Gustav Mie (1869–1957) proposed solutions (Mie's theory) to Maxwell's equations and described the scattering of light by perfectly spherical particles with diameter comparable to wavelength. As per Mie's theory, the phase shifts of scattered light from a particle depend on the difference in RIs of the particle and external medium. This makes it difficult to calculate the angular dependence of scattered light. To address this issue, the RGD (Rayleigh–Gans–Debye) approximation has emerged. In the RGD model, the scattering of light depends on three factors: (1) size of the particle; (2) wavelength of incident light; and (3) ratio of RIs of the particle and external medium. The wavelength of the scattered light is often different from the incident light after interaction with bigger particles due to factors like absorption and thus becomes inelastic (e.g., Raman and Brillouin scattering). Due to Doppler effect, the wavelength of scattered light in dynamic light scattering (DLS) is different from the wavelength of incident light. However, this difference in wavelengths is extremely small. Therefore, DLS is also known as QELS (quasi-elastic light scattering), although some literature still categorizes DLS as inelastic scattering. It is independent of zeta potential in terms of light scattering, but dependent on the RIs and also dependent on the particle size. We have found that there are no more differences in RIs from Cur-SN1 to Cur-SN9 i.e., 1.416–1.489. Therefore, RIs have no more effect in terms of light scattering and showed RIs near that of water (1.441). Therefore it is an indication of the transparent nature and oil-in-water (o/w) type behavior of all Cur-SNEDDS. (Bhattacharjee 2016).

Percentage transmission estimation is also useful to determine the transparent behavior of the developed SNEDDS. The percentage transmission of the developed formulations (Cur-SN1–Cur-SN9) was recorded as 92.46–99.08% (Table 4). The formulation Cur-SNEDDS (Cur-SN4) exhibited a maximum value of %transmission (99.08 ± 0.07%), whereas the formulation Cur-SNEDDS (Cur-SN6) exhibited the smallest value of % %transmission (92.46 ± 0.08%). All these results showed the transparent behavior of all Cur-SNEDDSs. But Cur-SNEDDS (Cur-SN4) was selected for the in vivo study because of the optimized size, PDI, median lowest zeta potential, lowest viscosity and refractive index as per the range for most stable nanoformulation as per our

previous study (Ahmad et al. 2017a, b, 2018a, b, c), and also having a maximum % transmittance. The small size of particles, i.e., < 20−30 nm, will cause their aggregation generally, and this aggregation produces a large particle size. Therefore, we have selected the optimum range of particle size > 50 nm, i.e., 59.56 ± 0.94 nm, followed by optimized PDI, i.e., 0.207 (Fig. 3a) to avoid the aggregation of particles or clumping of the particles. The graph in Fig. 3b shows a zeta potential of − 21.41 mV for optimized Cur−SNEDDS (Cur-SN4) and as per the previous reported studies the non-ionic surfactant-stabilized oil droplets allow a magnitude of droplet charge (Ahmad et al. 2018a, b). SEM and TEM were used to determine the shape and surface texture of the formulations. SEM images showed the smooth and round surface of Cur-SNEDDS (Cur-SN4) (Fig. 3c). TEM estimation was performed to find out the morphological behavior of the optimized Cur-SNEDDS (Cur-SN4). Cur-SN4 TEM images were observed and estimated for their surface morphology and droplet size (Fig. 3d). Cur-SN4 TEM images showed all droplets sizes within the nanometer range (Fig. 3d). Cur-SN4 SNEDDS showed the spherical shape of the droplets that can be due to the presence of eucalyptus oil and Tween 80 (Ahmad et al. 2017a, b, 2018a, b, c).

Differential scanning calorimetry (DSC)

According to the COA, the procured curcumin melting point range was observed 184–190 °C. Cur showed the sharp endothermic peak at 186.0 °C at the time of DSC analysis (Fig. 4), confirming the crystalline structure for curcumin. Some other DSC of Tween 80 (115.8 °C), Transcutol HP, showed many peaks between the 140 and 210 °C, and eucalyptus oil (153.91 °C, and 318.67 °C). Optimized Cur-SNEDDS (Cur-SN4) showed four very small peaks for eucalyptus oil, Transcutol HP, and Tween 80 in the thermogram of DSC. There was no peak for curcumin in the Cur-SNEDDS (Cur-SN4) DSC thermogram. This means Cur was completely entrapped inside the core of SNEDDS.

Analysis by ATR-based FT-IR

Pure curcumin, Tween 80, eucalyptus oil, Transcutol HP, and curcumin-self-nanoemulsifying drug delivery systems (Cur-SNEDDS) were characterized by FT-IR spectrophotometer which has been presented in Fig. 5. Pure curcumin, Tween 80, eucalyptus oil, Transcutol HP, and curcumin-self-nanoemulsifying drug delivery systems (Cur-SNEDDS)
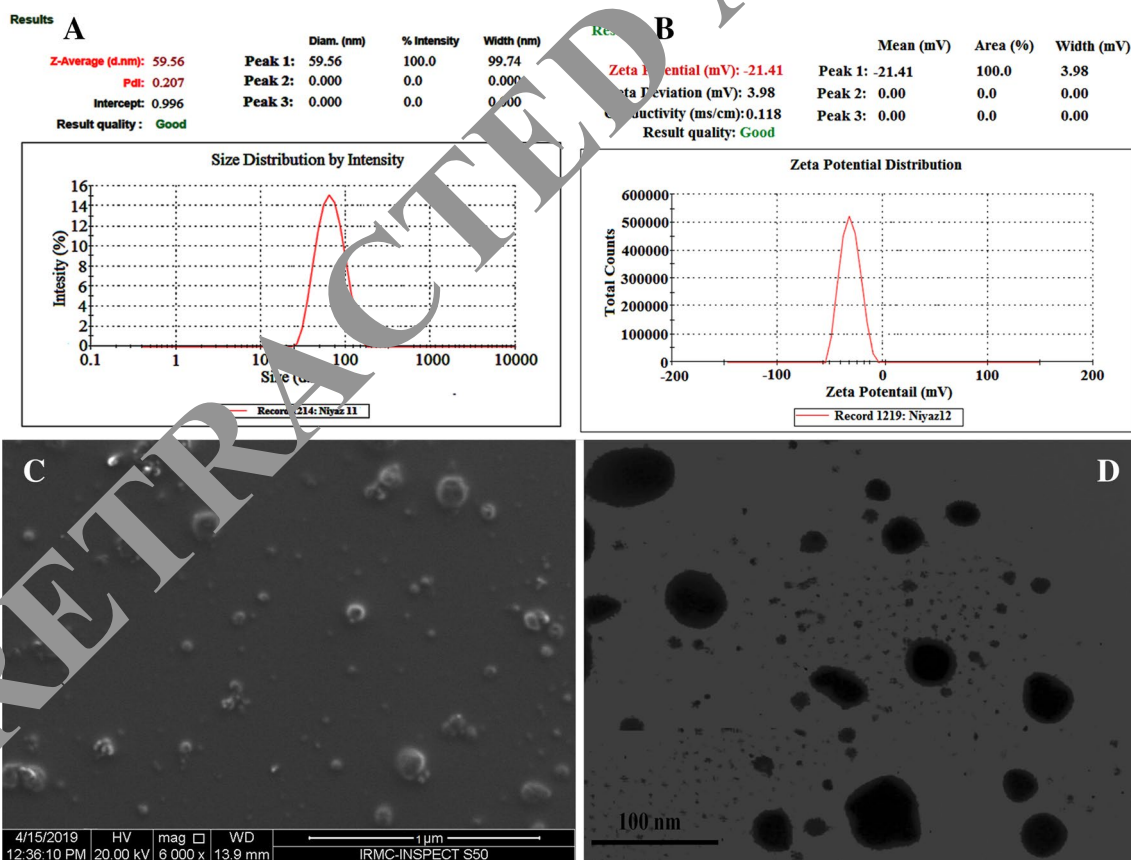

Fig. 3 Dynamic light scattering techniques for determining the particle size distribution of Cur-NE (**a**), zeta potential of Cur-SNEDDS (**b**), scanning electron microscopy (SEM) (**c**), and transmission electron microscopy (TEM) (**d**) images
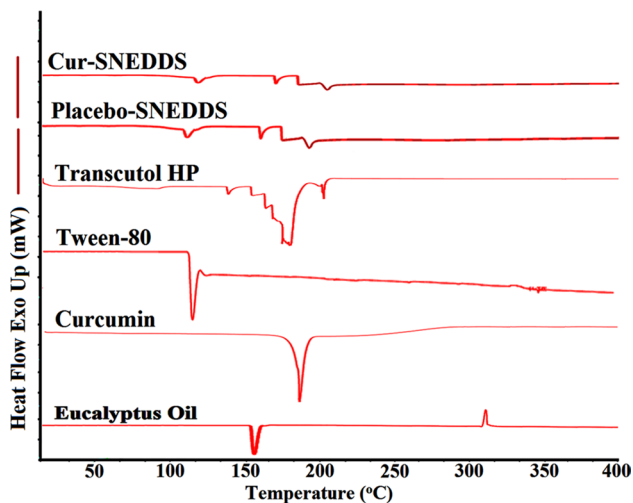
Fig. 4 Endothermic DSC thermograms of eucalyptus oil, pure curcumin, Tween 80, Transcutol HP, placebo-SNEDDS, and lyophilized-optimized Cur-SNEDDS
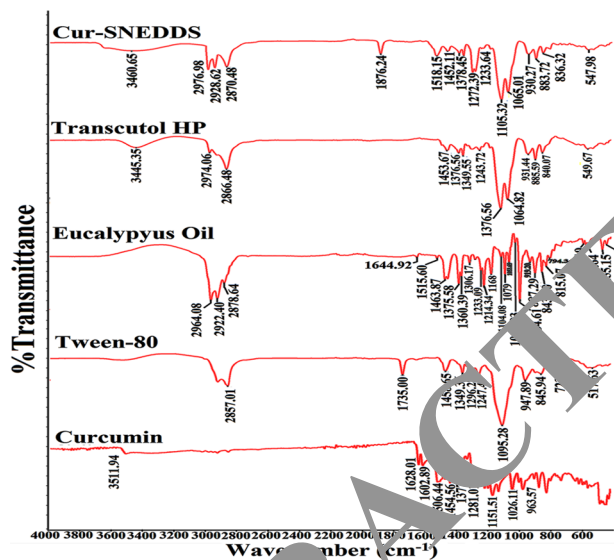

Fig. 5 FT-IR spectrum of curcumin, Tween 80, eucalyptus oil, Transcutol HP, and Cur-SNEDDS

were determined through ATR-based FT-IR spectroscopy. Nanomaterial surfaces were characterized by the ATR-based FT-IR spectroscopy which is a multipurpose tool that can be utilized both qualitatively and quantitatively (Wan et al. 2018; Ahmad et al. 2018d, 2019b). Curcumin showed their characteristic stretching band of O−H at 3511.95 cm^{-1}; 1628.01, C=C symmetric aromatic ring stretching at 1602.89; 1506.44, 1454.56, 1377.14, for C=O, while enol C−O peak was obtained at 1281.01; 1151.51, 1026.11, for benzoate trans-C−H vibration was at 963.57 cm^{-1}. Tween 80 showed characteristics peaks at 2857.01, 1735, 1458.65, 1426, 1349.36, 1296.27, 1247.49, 1095.28, 947.89, 845.94,

723.54, and 517.63 cm^{-1}. Eucalyptus oil showed characteristics peaks at 2964.08, 2922.40, 2878.64, 1644.92, 1515.60, 1463.87, 1375.58, 1360.39, 1306.17, 1233.09, 1214.34, 1168, 1104.08, 1079, 1014.83, 984.61, 919.20, 887.20, 843.10, 815.07, 794.34, 576.19, 543.64, 455.15, and 428.56 cm^{-1}. Transcutol HP showed characteristics peaks at 3445.35, 2974.06, 2866.48, 1453.67, 1376.56, 1064.82, 931.44, 885.59, 840.07, and 549.67 cm^{-1}. In the spectrum of Cur-SNEDDS, strong absorption bands at 3460.65, 2976.98, 2928.62, 2870.48, and 1876.24 cm^{-1} were observed and clearly indicated the entrapment of curcumin in the SNEDDS. The presence of OH stretching of Transcutol HP and the stronger intensity of this peak than curcumin were partly attributed to the hydrogen bonding between curcumin and Transcutol HP. Cur-SNEDDS achieved all the characteristic peaks of SNEDDS. But Cur characteristic peak in the Cur-SNEDDS was not found. This is due to ATR-FTIR spectroscopy analyzed the nanomaterial surfaces. It is clear indication curcumin was maximum encapsulated in the core of Cur-SNEDDS. Although a small amount of curcumin may be present on the surface of SNEDDS, Cur-amount was insignificant to be detected in comparison to Cur-SNEDDS. Finally, it was clearly indicated that there was no possible chemical reaction between curcumin and any one of the nanoformulation ingredients (Wan et al. 2018; Ahmad et al. 2018, 2019b; Inugala et al. 2015). Furthermore, it was more confirmed that the maximum curcumin was present inside the core of the SNEDDS. This is also an ignorance of the isomerization produced through light to facilitate stability and biological activities of curcumin.

In vitro drug release studies

In Fig. 6a, Cur-S was in vitro released initially at 30 min 70.33%, followed by 100% released at 2.0 h. On the other side, in vitro release profile (Fig. 6a) of Cur from optimized Cur-SNEDDS was observed in the biphasic phase with an initial burst release (26.33 ± 2.16% in 1.0 h), followed by sustained release. Finally, Cur was released from Cur-SNEDDS 75.94% attaining up to 78.49%. Curcumin burst was released initially from Cur-SNEDDS because of the Cur eroded outer layer from the Cur-SNEDDS. Finally, Cur present inside the core of the SNEDDS, i.e., lipid based which may be responsible for a sustained release profile (Nazari-Vanani et al. 2017; Inugala et al. 2015). Cur-release kinetics was observed to fit in the many models from optimized Cur-SNEDDS, in which the maximum R^2 value was accepted as the most excellent model for release of Cur from Cur-SNEDDS nanoformulation for the in vitro drug release model. Higuchi model showed an $R^2 = 0.9861$ which was the maximum value. The first order gave the correlation coefficient (R^2), i.e., 0.9703, and then we observed the zero order ($R^2 = 0.9231$), followed by Korsmeyer–Peppas. This
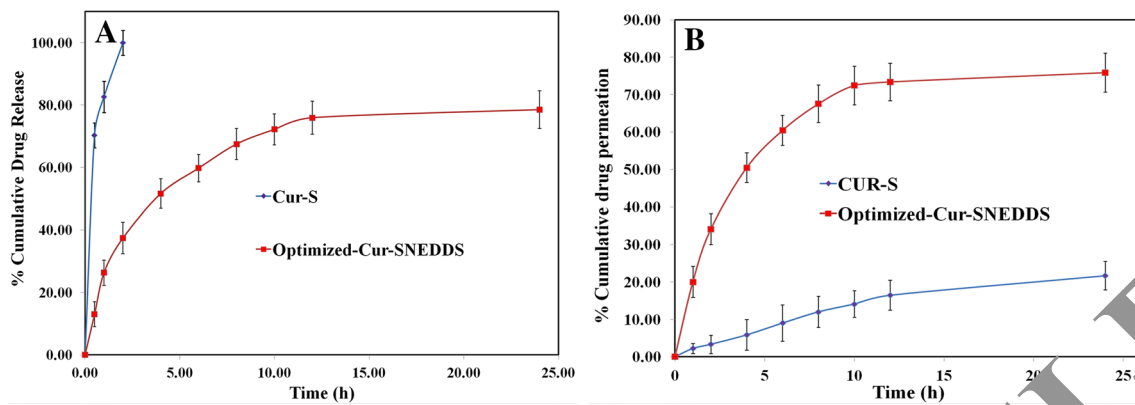
Fig. 6 **a** The cumulative percentage release of curcumin from Cur-SNEDDS as compared to pure curcumin. **b** In vitro skin permeation profiles of developed Cur-SNEDDS as compared to pure curcumin through rat skin

study was essential to show the initial burst release of Cur, followed by a sustained release to attain the maximum concentration gradient involved in the successful transdermal drug delivery of Cur (Ahmad et al. 2018a, b).

In vitro skin permeation study

The rat skin was isolated for Cur-pure suspension form optimized Cur-SNEDDS for the permeation studies (Fig. 6b). The cumulative drug permeation of the Cur study showed permeation for Cur-suspension ($21.67 \pm 3.54\%$) and optimized Cur-SNEDDS ($75.89 \pm 5.19\%$) after 24.0 h. In the optimized Cur-SNEDDS, Tween 80 surfactant existed in polysorbate form, thus it had the ability to improve the drug permeation through penetrating into the intracellular regions of the stratum corneum and ultimately solubilize lipid components (El-Say et al. 2015; Badran et al. 2014; Yan et al. 2011). The maximum solubility of curcumin was found in Tween 80 and Transcutol HP. Tween and Transcutol HP were mixed and facilitated enhancing the emulsifying stability of Tween 80. Moreover, both Tween 80 and Transcutol HP participated as bioavailability enhancers (Ahmad et al. 2018a, b; Yan et al. 2011). Thus, Tween 80 and Transcutol HP were selected as the surfactant and co-surfactant for more examination.

SNEDDS is a novel drug delivery system with numerous advantages including ease of production and improvement of drug solubility and bioavailability. SNEDDSs are preconcentrates composed of isotropic mixtures of oils, surfactants and co-surfactants, which spontaneously form fine oil in water (o/w) emulsion in situ upon contact through aqueous medium with a globule size in the range of 20–200 nm (Pouton and Porter 2008). It is an anticipated technology to increase the water solubility of poorly water-soluble drugs due to their large solubilization capacity and small droplet size. These properties of SNEDDS allow enhanced

permeation and bioavailability of the formulated drug across the skin membrane (Badran et al. 2014).

The ex vivo permeations study showed the enhanced permeation of the encapsulated Cur from Cur-SNEDDS as a result of improved solubility, and consequently the thermodynamics of the system, through the skin layers into the systemic circulation. In addition, nanoemulsions and SNEDDS applied to the skin could potentially penetrate the stratum corneum, altering both lipid and polar pathways of drug absorption by the virtue of its oily and surfactant content (Pacharodi and Panduranga Rao 1994; El-Say et al. 2015). This alteration in the penetration pathways could allow lipophilic drugs such as Cur to permeate more easily through the stratum corneum barrier, thus explaining the enhanced permeation of Cur from Cur-SNEDDS compared with Cur-S. In addition, the small formed droplet size in the nano range could make SNEDDS an efficient carrier for enhancing percutaneous penetration of Cur owing to increased number of vesicles that can interact on a fixed area of stratum corneum with the decrease in droplet size (Pathan and Setty 2011; El-Say et al. 2015). Furthermore, surfactants (non-ionic surfactant act as a permeation/penetration enhancer, e.g., Tween 80 and Transcutol HP), which can loosen or fluidize the lipid bilayers of the stratum corneum, can act as permeation enhancers. Compared to microemulsions, transdermal nanoemulsions have been shown to increase the bioavailability and efficacy of compounds such as anti-inflammatory agents (Elnaggar Yosra et al. 2011).

Pharmacodynamic study

Wound healing evaluation

Wound healing images of the control group (placebo): optimized nanoemulsion without Cur loaded; pure eucalyptus

oil; pure Cur-S; optimized Cur-SNEDDS and marketed preparation of antibiotic fusidic acid (brand name: Fusidin; positive control) on wound area contraction for rats are shown in Fig. 7. However, the results of the effects of pure eucalyptus oil, pure Cur-S, optimized Cur-SNEDDS and marketed preparation of antibiotic fusidic acid (brand name: Fusidin; positive control) on wound area contraction of rats are shown in Fig. 8. These results exhibited that wound contraction of rats was improved till day 24 in all three test samples (pure eucalyptus oil; pure Cur-S; optimized Cur-SNEDDS) and fusidic acid-treated rats. Pure eucalyptus oil and pure Cur-S significantly helped in the wound contraction since day 12–24 when compared to the control group ($P < 0.05$). Cur-NE and fusidic acid significantly helped in wound contraction since day 12–24 compared to the control group ($P < 0.01$) in Fig. 8. Cur-SNEDDS showed the same effects on the treatment of wound healing in comparison to fusidic acid due to their nanosize particle and enhancement of penetration, followed by a more sustained released action. It may be due to the additive action of eucalyptus oil. The results of the effect of tests (pure eucalyptus oil, pure Cur-S and Cur-SNEDDS) as compared to antibiotic fusidic acid on the epithelization period are shown in Fig. 9.
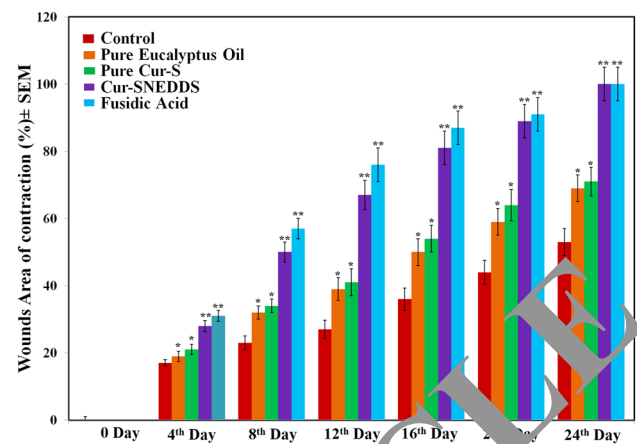

Fig. 8 Influence of oral administration: control group: optimized nanoemulsion without Cur loaded; pure eucalyptus oil; pure Cur-S; optimized nanoemulsion and marketed preparation of antibiotic fusidic acid (brand name: Fusidin serves as positive control on circular excision wound model in rats at different days of treatment. *$P < 0.05$ as compared to control
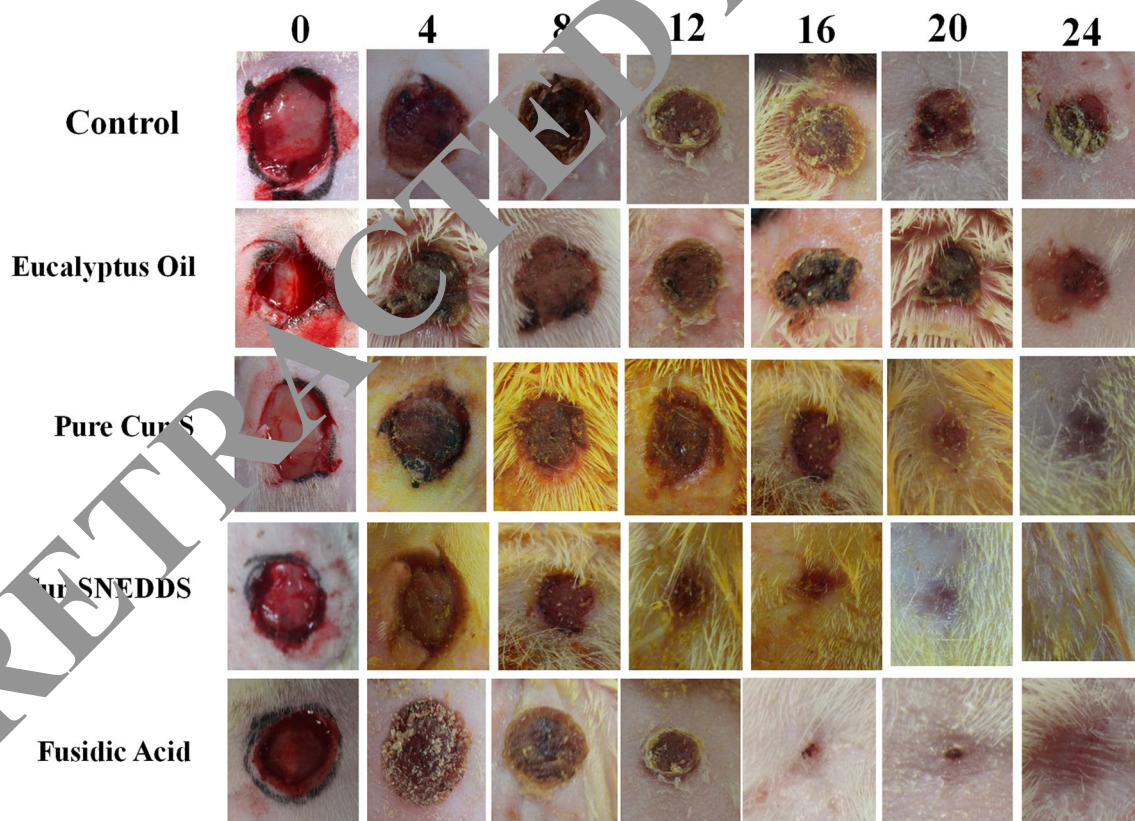

Fig. 7 Wound healing effects of control group: optimized nanoemulsion without Cur loaded; pure eucalyptus oil; pure Cur-S; pure Cur-SNEDDS; optimized nanoemulsion and marketed preparation of antibiotic fusidic acid (brand name: Fusidin serves as positive control) in comparison with control after 0, 4, 8, 12, 16, 20 and 24 days of inducing wound healing

The complete epithelization time was achieved at 21 ± 1, 17 ± 1, 17.3 ± 1, 9.5 ± 0.7 and 9.5 ± 0.7 day for control (placebo), pure eucalyptus oil, pure Cur-S and Cur-SNEDDS and antibiotic fusidic acid, respectively. The epithelization period was adequately smaller in Cur-SNEDDS and antibiotic fusidic acid-treated rats when compared to the control, pure eucalyptus oil, and pure Cur-S-treated rats ($P < 0.05$). The effects of wound contraction and epithelization for Cur-SNEDDS were extremely comparable with antibiotic fusidic acid. It was found that the results for pure eucalyptus oil and pure Cur-SNEDDS were highly efficacious in SNEDDS in comparison with its pure form. On the basis of these results, the optimized Cur-SNEDDS exhibited maximum wound healing effects after topical application as compared to pure eucalyptus oil and pure Cur-S. The increased wound contraction through Cur-SNEDDS was possible due to nano-range droplets of SNEDDS and the presence of penetration enhancers and solubilizers such as Tween 80 and Transcutol HP in Cur-SNEDDS. The potential of producing wound contraction by pure eucalyptus oil, pure Cur-S, and Cur-SNEDDS obtained in this study indicated that pure eucalyptus oil and pure Cur-S plant contain a definite pro-healing action, as 100.0% of wound healing was found that indicated contraction (Fitzmaurice et al. 2011; Thomas et al. 2017; Gopinath et al. 2004; Sidhu et al. 1998; Gong et al. 2013). These results of wound healing for pure eucalyptus oil, pure Cur-S, and Cur-SNEDDS were probably due to a particular increment in the proliferation of epithelial cells (Sidhu et al. 1998). The most important outcome of the current research was that pure eucalyptus oil, pure Cur-S, and Cur-SNEDDS applied topically accelerated the wound healing effects with greater and faster rate in the developed rat's excision wound model.

The current proposed research outcomes showed that the topical application of pure eucalyptus oil, pure Cur-S, and
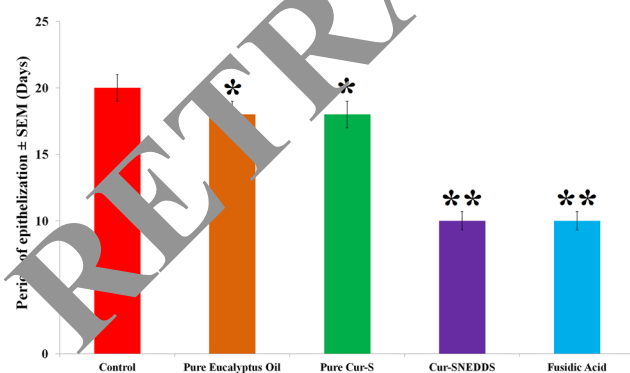

Fig. 9 Influence of oral administration of control group: optimized nanoemulsion without Cur loaded; pure eucalyptus oil; pure Cur-S; optimized nanoemulsion and marketed preparation of antibiotic fusidic acid (brand name: Fusidin serves as positive control on wound epithelization period. *$P < 0.01$ as compared to control

Cur-SNEDDS, given one time a day for 24 days, enhanced the rate of wound closure in excision wound model for the rats. Curcumin healed wounds followed by essential oils have been examined in literature on animal models (Gopinath et al. 2004; Sidhu et al. 1998; Thomas et al. 2017; Kumar et al. 2007; de Fatima et al. 2008; Tumen et al. 2011; Suntar et al. 2011). On the basis of previously reported literature, the injured tissues were re-established and functionally worked as before. This involved many steps such as "wound contraction, inflammation, angiogenesis, extracellular matrix deposition and tissue reformation". Wound healing has single/multiple mechanisms to complete the wound healing process (Velnar et al. 2009; Gheb et al. 2011). Optimized Cur-SNEDDS was observed to reduce the swelling and exudates in the rats at every 4th day post-wounding. All the effects of wound healing were evaluated and found to be comparable to those of standard fusidic acid-treated animals and higher than those of control, pure eucalyptus oil, and pure Cur-S treated animals (Fig. 7).

The main objective of the current research study was to develop a novel SNEDDS of Cur to increase their wound healing effects. Here SNEDDS are lipid-based preparations that are best formulations for greater potency, followed by poor water solubility of Cur (Porter et al. 2007; Singh et al. 2009). Transdermal drug delivery of SNEDDS has been reported previously (Villar et al. 2012). This system has the most important advantage of having the highest stability of the hydrolyzable drug. This was commonly seen that SNEDDS has been transformed into nanoemulsion when mixed with aqueous phase approaching from the skin followed by occlusive topical application. Supersaturated system was found while a result of this dilution. Thus, higher driving force was obtained for transdermal drug delivery (Porter et al. 2007; Singh et al. 2009; Villar et al. 2012). A novel Cur-SNEDDS were prepared and optimized that are clear, isotropic system of drug, transparent, surfactant, oil, and co-surfactant. It will form ultra-fine nanoemulsions (generally < 100 nm in size) for the less agitation and making the dilution by aqueous medium (Villar et al. 2012; Thomas et al. 2012). For transdermal delivery of the Cur, Cur-loaded SNEDDS has been used for the first time as a nanocarrier. We applied topically Cur-loaded SNEDDS that is spread simply on the surface of the skin. It was mixed easily with transepidermal water loss giving the curcumin in the range of nanosize which is responsible for improving the curcumin dissolution and skin permeation. Thus, Cur-loaded SNEDDS is also utilized to improve the solubility as well as dissolution rate of Cur and decrease their side effects related to oral drug delivery (Taha et al. 2015). SNEDDS-based preparations enhanced the skin permeation by the mechanism, i.e., enhanced aqueous phase upon dilution and after that decreased the drug solubility. It have given a supersaturated nanoemulsion system (in situ) that improves the drug

thermodynamic activity, followed by high driving force for transdermal delivery (Taha et al. 2015; El Maghraby 2008). In the preparation of Cur-loaded SNEDDS, the use of surfactants enhanced the transdermal delivery of the curcumin compared to Cur-S significantly. Transcutol HP and Tween 80 provided a great improvement in the transdermal delivery of curcumin. As a result, the improved wound healing effects of Cur-SNEDDS were observed possibly due to enhancement in skin permeation or delivery of Cur from SNEDDS.

Wound healing tissues evaluation by histopathology

Histopathological image evaluation of the control group (placebo), tests (pure eucalyptus oil, pure Cur-S, and Cur-loaded SNEDDS) and reference fusidic acid-treated rats are shown in Fig. 10. On the 12th day, histological examination of skin with H&E exhibited signs of edema, ulceration, granulation, epithelization, and large quantity of mononuclear cell infiltration in the rats (control group) (Fig. 10a). On the other hand, pure eucalyptus oil and pure Cur-S treated rat's images illustrated marks of edema, less ulceration, and a great quantity of granulation as well as also the indications of healed skin structure with more formed, close to normal epidermis, restoration of adnexa, and extensive fibrosis and collagen tissue within the dermis (Fig. 10b, c). Rats treated

with Cur-SNEDDS exhibited a huge quantity of granulation tissue, a small number of mononuclear inflammatory cells, and re-establishment of adnexa and large area of fibrosis and no other indication of ulceration and edema (Fig. 10d). Rats treated with reference group: antibiotic fusidic acid exhibited healed skin structures with best-recovered very closed to standard epidermis, large area of fibrosis and collagen tissue within the dermis, and re-establishment of adnexa (Fig. 10e). Histopathological final analysis data are shown in Fig. 11. On the basis of the above observation, pure eucalyptus oil and pure Cur-S repaired and healed the wounds clearly. On the basis of the above data analysis basically when compared to other plants, pure eucalyptus oil and pure Cur-S are renowned for their antibacterial, antioxidant, antifungal, and anti-inflammatory activity (Alam et al. 2018; Gopinath et al. 2004; Sidhu et al. 1998). Therefore, we concluded that oxidative stress reduction plays a very great role in wound healing (Yusufoglu and Alqasoumi 2011; Alam et al. 2018; Sidhu et al. 1998).

Anti-inflammatory activity

Inflammation was developed by rat hind paw edema model for the current research study (Ahmad et al. 2018a; Winter et al. 1963). Inflammagen were taken carrageenan injected to develop the edema. Cur-SNEDDS exhibited significant
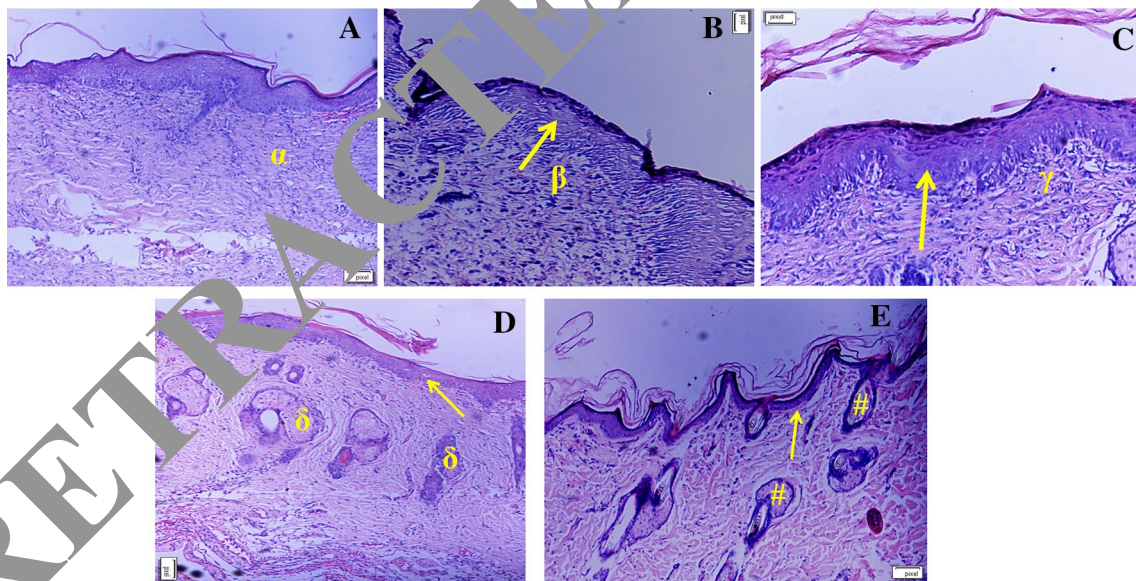

Fig. 10 Histopathology of skin at day 12 stained with H&E; **a** control group animals showing, early epithelization, and granulation tissue and abundance of mononuclear inflammatory cells (α); **b** pure eucalyptus oil-treated rats showing healed skin structures with well-formed, near to normal epidermis, restoration of adnexa (β), and extensive fibrosis and collagen tissue within the dermis (arrow); **c** pure curcumin-treated rats showing healed skin structures with well-formed, near to normal epidermis, restoration of adnexa (γ), and extensive fibrosis and collagen tissue within the dermis (arrow); **d** Cur-SNEDDS-treated rats showing large amount of granulation tissue, small number of mononuclear inflammatory cells, and restoration of adnexa and extensive fibrosis (δ); **e** Fusidic acid-treated rats showing healed skin structures with well-formed, near to normal epidermis, restoration of adnexa, and extensive fibrosis and collagen tissue within the dermis (#)
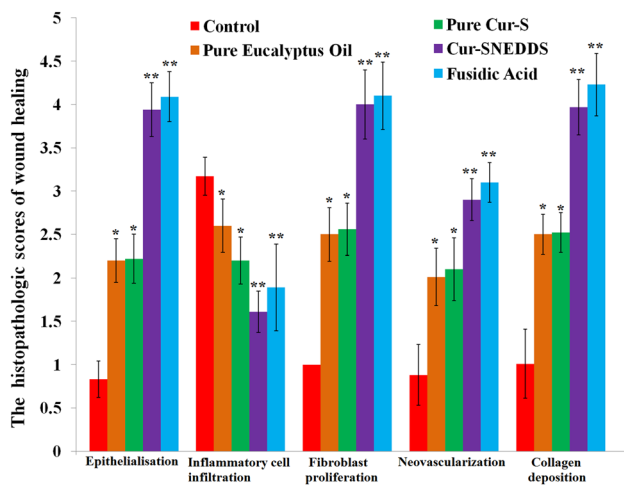
Fig. 11 The median histopathological scores of wound healing determined after topical application of control group: optimized nanoemulsion without Cur loaded; pure eucalyptus oil; pure Cur-S; optimized nanoemulsion and marketed preparation of antibiotic fusidic acid (brand name: Fusidin serves as positive control by using a modified 0–4 numerical scale; the scores were 0 for absence, 1 for occasional presence, 2 for light scattering, 3 for abundance, and 4 for confluence of cells or fibers. $*P < 0.05$ and $**P < 0.01$ as compared to control

reduction ($p < 0.05$) in inflammation (47.98%) in comparison of pure Cur-S (13.16%) in the rats. Cur-SNEDDS showed better results in the treatment of inflammation in the rat's paw significantly.

Molecular evidence for the involvement in wound healing consists of inhibiting cell mobility, cell proliferation, producing antioxidant activity, and coordinating metabolism (Hsiao et al. 2012). In general, wound healing is an orderly complex process that consists of overlapping phases; inflammatory reaction, cellular phase (granulation), narrowing of wound area (wound contraction), collagen deposition (collagen formation), epithelial covering (epithelialization), and scar remodeling (cicatrization). The inflammatory phase involves vascular responses characterized by exudation, blood coagulation, and hemostasis. During this process, varieties of immune cells from the blood vessels are attracted to the wound lesion and secrete pro-inflammatory cytokines. The inflammatory cells, notably neutrophils, may produce large amounts of reactive oxygen species (ROS). The ROS are essential in protecting the body against developing infection, but, when present in excess amount, can simultaneously damage the surrounding tissues (Lazarus et al. 1994; Nagori and Solanki 2011; Gebremeskel et al. 2018; Kurahashi and Fujii, 2015; Ibrahim et al. 2018; Ahmad et al. 2018a; Alam et al. 2017, 2018).

Curcumin has been reported to have a potential role in the antioxidant activity with a great effect on the immune cells and inflammatory cytokines (Ahmad et al. 2013, 2016b;

Thomas et al. 2017). We discuss the other mechanism here that curcumin-loaded SNEDDS prevents wound injury by ameliorating oxidative damage. Cur-loaded SNEDDS nanoformulation also plays an important role in the process of wound healing, a reduction of immune cells and inflammatory cytokines and migrating keratinocytes, fibroblasts, and endothelial cells (Fig. 11, 10). Subsequently Cur-loaded SNEDDS nanoformulation also plays an important role during the proliferative phase; it helps in the formation of the epithelium to cover the wound surface with concomitant growth of granulation tissue to fill the space of wound (Figs. 7, 10, 11). Cur-loaded SNEDDS nanoformulation helps in the formation of granulation tissue involves proliferation of fibroblasts, deposition of collagens and other extracellular matrices (ECM) and development of new blood vessels (angiogenesis) (Figs. 11). In this way, the collagen synthesis causes contraction of wound and reduction of the wound size (Figs. 7). The temporal ECM is gradually converted into a mature scar. This remodeling process will restore tissue structural integrity and functional competence. The process of wound healing is tightly regulated by multiple growth factors and cytokines released at the wound site (Ahmad et al. 2018a; Alam et al. 2017, 2018; Kurahashi and Fujii 2015; Ibrahim et al. 2018). Finally, the authors provide a feasible and effective tool that can be used for the study of the molecular basis of traditional herbal medicines.

Conclusion

Cur-loaded SNEDDS nanoformulation showed improved wound healing effects potentially in this study. Optimized Cur-loaded SNEDDS nanoformulation was characterized physicochemically and related to wound healing examination in rats with comparison to reference fusidic acid, pure eucalyptus oil, and pure Cur-S. Cur-loaded SNEDDS effects on wound healing were seen to be significant compared with those of pure eucalyptus oil, pure Cur-S, and control. But all the effects were very comparable with standard fusidic acid. Furthermore, Cur-loaded SNEDDS histopathological evaluations of treated rats exhibited no signs of inflammatory cells and showed that the optimized Cur-loaded SNEDDS was safe and nontoxic for rats. For topical delivery of curcumin, Cur-loaded SNEDDS showed improved wound healing effects in rats. On the other hand, eucalyptus oil healed the wounds successfully in this study. Hence, the combination of curcumin and eucalyptus oil, particularly in the form of nanoformulation (SNEDDS), would be the best way to treat faster wound healing in the future. In parallel, the developed and optimized Cur-SNEDDS was highly effective than pure Cur-S in the healing of edema and showed anti-inflammatory activity in the carrageenan-induced rat paw edema model.

References

Ahmad N, Umar S, Ashafaq M, Akhtar M, Iqbal Z, Samim M, Ahmad FJ (2013) A comparative study of PNIPAM nanoparticles of curcumin, demethoxycurcumin, and bisdemethoxycurcumin and their effects on oxidative stress markers in experimental stroke. Protoplasma 250(6):1327–1338. https://doi.org/10.1007/s00709-013-0516-9

Ahmad N, Ahmad R, Alam MA, Samim M, Iqbal Z, Ahmad FJ (2016a) Quantification and evaluation of thymoquinone loaded mucoadhesive nanoemulsion for treatment of cerebral ischemia. Int J Biol Macromol 88:320–332. https://doi.org/10.1016/j.ijbiomac.2016.03.019

Ahmad N, Ahmad I, Umar S, Iqbal Z, Samim M, Ahmad FJ (2016b) PNIPAM nanoparticles for targeted and enhanced nose-to-brain delivery of curcuminoids: UPLC/ESI-Q-ToF-MS/MS-based pharmacokinetics and pharmacodynamic evaluation in cerebral ischemia model. Drug Deliv 23(7):2095–2114. https://doi.org/10.3109/10717544.2014.941076

Ahmad N, Ahmad R, Naqvi AA, Alam MA, Abdur Rub R, Ahmad FJ (2017a) Enhancement of quercetin oral bioavailability by self-nanoemulsifying drug delivery system and their quantification through ultra high performance liquid chromatography and mass spectrometry in cerebral ischemia. Drug Res (Stuttg) 67(10):564–575. https://doi.org/10.1055/s-0043-109564

Ahmad N, Ahmad R, Naqvi AA, Alam MA, Ashafaq M, Iqbal Ahmad FJ (2017b) Isolation, characterization and quantification of curcuminoids and their comparative effects in cerebral ischemia. J Liq Chromatogr Relat Technol 40(3):133–147. https://doi.org/10.1080/10826076.2017.1293559

Ahmad N, Ahmad R, Alam MA, Ahmad FJ, Amir M (2018a) Impact of ultrasonication techniques on the preparation of novel Amiloride-nanoemulsion used for intranasal delivery in the treatment of epilepsy. Artif Cells Nanomed Biotechnol 46(sup3):S192–S207. https://doi.org/10.1080/21691401.2018.1489826

Ahmad N, Ahmad R, Al-Qudaihi A, Al-shawi H, Al-ali A, Amir M, Mostafa A (2018b) Ultra-high performance liquid chromatography-based identification and quantification of thymoquinone in Nigella sativa extract from different geographical regions. Pharmacogn Mag 14(57):S471-S48. https://doi.org/10.4103/pm.pm_119_18

Ahmad N, Alam MA, Ahmad FJ, Sarafroz M, Ansari K, Sharma S, Amir M (2018c) Ultrasonication techniques used for the preparation of novel Eugenol-Nanoemulsion in the treatment of wounds healings and anti-inflammatory. J Drug Deliv Sci Technol 46:461–473. https://doi.org/10.1016/j.jddst.2018.06.003

Ahmad N, Ahmad R, Naqvi AA, Alam MA, Ashafaq M, Abdur Rub R, Ahmad FJ (2018d) Intranasal delivery of quercetin-loaded mucoadhesive nanoemulsion for treatment of cerebral ischaemia. Artif Cells Nanomed Biotechnol 46(4):717–729. https://doi.org/10.1080/21691401.2017.1337024

Ahmad N, Ahmad R, Alam MA, Ahmad FJ, Amir M, Pottoo FH, Sarafroz M, Jafar M, Umar K (2019a) Daunorubicin oral bioavailability enhancement by surface coated natural biodegradable macromolecule chitosan based polymeric nanoparticles. Int J Biol Macromol 128:825–838. https://doi.org/10.1016/j.ijbiomac.2019.01.142

Ahmad N, Ahmad FJ, Bedi S, Sharma S, Umar S (2019b) A novel nanoformulation development of eugenol and their treatment in inflammation and periodontitis. Saudi Pharm J. https://doi.org/10.1016/j.jsps.2019.04.014

Alam P, Ansari MJ, Anwer MK, Raish M, Kamal YK, Shakeel F (2017) Wound healing effects of nanoemulsion containing clove essential oil. Artif Cells Nanomed Biotechnol 45(3):591–597. https://doi.org/10.3109/21691401.2016.1163716

Alam P, Shakeel F, Anwer MK, Foudah AI, Alqarni MH (2018) Wound healing study of eucalyptus essential oil containing nanoemulsion in rat model. J Oleo Sci 67(8):957–968. https://doi.org/10.5650/jos.ess18005

Al-Rohaimi AH (2015) Comparative anti-inflammatory potential of crystalline and amorphous nano curcumin in topical drug delivery. J Oleo Sci 64(1):27–40. https://doi.org/10.5650/jos.ess14175

Badran MM, Taha EI, Tayel MM, Al-Suwayeh SA (2014) Ultra-fine self nanoemulsifying drug delivery system for transdermal delivery of meloxicam: dependency on the type of surfactants. J Mol Liq 190:16–22. https://doi.org/10.1016/j.molliq.2013.10.015

Bhattacharjee S (2016) DLS and zeta potential—what they are and what they are not? J Control Release 238:311–312. https://doi.org/10.1016/j.jconrel.2016.08.002

Boateng J, Catanzano O (2015) Advanced therapeutic dressing for effective wound healing—review. J Pharm Sci 104(11):3653–3680. https://doi.org/10.1002/jps.24610

Cirri M, Maestrini L, Maestrelli F, Mennini N, Mura P, Ghelardini C, Di Cesare Mannelli L (2018) Design, characterization and in vivo evaluation of nanostructured lipid carriers (NLC) as a new drug delivery system for hydrochlorothiazide oral administration in pediatric therapy. Drug Deliv 25(1):1910–1921. https://doi.org/10.1080/10717544.2018.1529209

Cássia da Silveira R, Andrade LN, de Sousa DP (2013) A Review on anti-inflammatory activity of monoterpenes. Molecules 18(1):1227–1254. https://doi.org/10.3390/molecules18011227

de Fatima A, Modolo LV, Sanches AC, Porto RR (2008) Wound healing agents: the role of natural and non-natural products in drug development. Mini Rev Med Chem 8:879–888. https://doi.org/10.2174/138955708785132738

El Maghraby GM (2008) Transdermal delivery of hydrocortisone from eucalyptus oil microemulsion: effects of cosurfactants. Int J Pharm 355(1–2):285–292. https://doi.org/10.1016/j.ijpharm.2007.12.022

Elnaggar Yosra SR, El-Massik Magda A, Abdallah Ossama Y (2011) Sildenafil citrate nanoemulsion vs. self-nanoemulsifying delivery systems: rational development and transdermal permeation. Int J Nanotechnol 8(8/9):749–763. https://doi.org/10.1504/IJNT.2011.041443

El-Say KM, Ahmed TA, Badr-Eldin SM, Fahmy U, Aldawsari H, Ahmed OAA (2015) Enhanced permeation parameters of optimized nanostructured simvastatin transdermal films: ex vivo and in vivo evaluation. Pharm Dev Technol 20(8):919–926. https://doi.org/10.3109/10837450.2014.938859

Fitzmaurice SD, Sivamani RK, Isseroff RR (2011) Antioxidant therapies for wound healing: a clinical guide to currently commercially available products. Skin Pharmacol Physiol 24(3):113–126. https://doi.org/10.1159/000322643

Gebremeskel L, Bhoumik D, Sibhat GG, Tuem KB (2018) In vivo wound healing and anti-inflammatory activities of leaf latex of aloe megalacantha baker (Xanthorrhoeaceae). Evid Based Complement Alternat Med 2018:5037912. https://doi.org/10.1155/2018/5037912

Ghosh V, Mukherjee A, Chandrasekaran N (2013) Ultrasonic emulsification of food-grade nanoemulsion formulation and evaluation of its bactericidal activity. Ultrason Sonochem 20(1):338–344. https://doi.org/10.1016/j.ultsonch.2012.08.010

Gong C, Wu Q, Wang Y, Zhang D, Luo F, Zhao X, Wei Y, Qian Z (2013) A biodegradable hydrogel system containing curcumin encapsulated in micelles for cutaneous wound healing. Biomaterials 34(27):6377–6387. https://doi.org/10.1016/j.biomaterials.2013.05.005

Gopinath D, Ahmed MR, Gomathi K, Chitra K, Sehgal PK, Jayakumar R (2004) Dermal wound healing processes with curcumin incorporated collagen films. Biomaterials 25(10):1911–1917. https://doi.org/10.1016/S0142-9612(03)00625-2

Gould L, Abadir P, Brem H et al (2015) Chronic wound repair and healing in older adults: current status and future research. J Am Geriatr Soc 63(3):427–438. https://doi.org/10.1111/jgs.13332

Grieb G, Steffens G, Pallua N, Bernhagen J, Bucala R (2011) Circulating fibrocytes—biology and mechanisms in wound healing and scar formation. Int Rev Cell Mol Biol 291:1–19. https://doi.org/10.1016/B978-0-12-386035-4.00001-X

Hsiao CY, Tsai TH, Chak KF (2012) The molecular basis of wound healing processes induced by lithospermi radix: a proteomics and biochemical analysis. Evid Based Complement Alternat Med 2012:508972. https://doi.org/10.1155/2012/508972

Ibrahim N, Wong SK, Mohamed IN, Mohamed N, Chin KY, Ima-Nirwana S, Shuid AN (2018) Wound healing properties of selected natural products. Int J Environ Res Public Health. https://doi.org/10.3390/ijerph15112360

Inugala S, Eedara BB, Sunkavalli S, Dhurke R, Kandadi P, Jukanti R, Bandari S (2015) Solid self-nanoemulsifying drug delivery system (S-SNEDDS) of darunavir for improved dissolution and oral bioavailability: in vitro and in vivo evaluation. Eur J Pharm Sci 74:1–10. https://doi.org/10.1016/j.ejps.2015.03.024

Jain S, Kambam S, Thanki K, Jain AK (2015) Cyclosporine A loaded self-nanoemulsifying drug delivery system (SNEDDS): implication of a functional excipient based co-encapsulation strategy on oral bioavailability and nephrotoxicity. RSC Adv 5:49633–49642. https://doi.org/10.1039/x0xx00000x

Jaiswal M, Dudhe R, Sharma PK (2015) Nanoemulsion: an advanced mode of drug delivery system. 3 Biotech 5:123–127. https://doi.org/10.1007/s13205-014-0214-0

Juergens UR, Dethlefsen U, Steinkamp G, Gillissen A, Repges R, Vetter H (2003) Anti-inflammatory activity of 1,8-cineol (eucalyptol) in bronchial asthma: A double-blind placebo-controlled trial. Respir Med 97(3):250-256

Khan AW, Kotta S, Ansari SH, Sharma RK, Ali J (2015) Self-nanoemulsifying drug delivery system (SNEDDS) of the poorly water-soluble grapefruit flavonoid Naringenin: design, characterization, in vitro and in vivo evaluation. Drug Deliv 22(4):552–561. https://doi.org/10.3109/10717544.2013.878003

Kumar B, Vijayakumar M, Govindarajan R, Pushpangadan P (2007) Ethnopharmacological approaches to wound healing—exploring medicinal plants of India. J Ethnopharmacol 114(2):103–113. https://doi.org/10.1016/j.jep.2007.08.010

Kurahashi T, Fujii J (2015) Roles of Antioxidative Enzymes in Wound Healing. J Dev Biol 3(2):57–70. https://doi.org/10.3390/jdb3020057

Lazarus GS, Cooper DM, Knighton DR, Percoraro RE, Rodeheaver G, Robson MC (1994) Definitions and guidelines for assessment of wounds and evaluation of healing. Wound Repair Regen 2(3):165–170. https://doi.org/10.1046/j.1524-475X.1994.20305.x

McClements DJ, Xiao H (2012) Potential biological fate of ingested nanoemulsions: influence of particle characteristics. Food Funct 3(3):202–220. https://doi.org/10.1039/c1fo10193e

Moghaddam AA, Ahad A, Aqil M, Ahmad FJ, Sultana Y, Ali A (2018) Ibuprofen loaded nano-ethanolic liposomes carbopol gel system: in vitro characterization and anti-inflammatory efficacy assessment in Wistar rats. J Polym Eng 38(3):291–298. https://doi.org/10.1515/polyeng-2016-0462

Monika Garg R, Sardana S (2018) Bioavalibility enhancement of Resveratrol using self nanoemulsifying drug delivery system developed applying central composite design. Int J Pharm Sci Res 9(8):3334–3346. https://doi.org/10.13040/IJPSR.0975-8232.9(8).3334-46

Nagori BP, Solanki R (2011) Role of medicinal plants in wound healing. Res J Med Plant 5(4):392–405. https://doi.org/10.3923/rjmp.2011.392.405

Nasr AM, Gardouh AR, Ghonaim HM, Ghorab MM (2016a) Design, formulation and in vitro characterization of Irbesartan solid self-nanoemulsifying drug delivery system (S-SNEDDS) prepared using spray drying technique. J Chem Pharm Res 8:159–183

Nasr A, Gardouh A, Ghorab M (2016b) Novel Solid Self-Nanoemulsifying Drug Delivery System (S-SNEDDS) for Oral Delivery of Olmesartan Medoxomil: design, formulation, pharmacokinetic and bioavailability evaluation. Pharmaceutics 8(3):E20. https://doi.org/10.3390/pharmaceutics8030020

Nazari-Vanani R, Moezi L, Heli H (2017) In vivo evaluation of a self-nanoemulsifying drug delivery system for curcumin. Biomed Pharmacother 88:715–720. https://doi.org/10.1016/j.biopha.2017.01.102

Nipun TS, Islam SMA (2014) SEDDS of gliclazide: preparation and characterization, in vitro, ex vivo and in vivo techniques. Saudi Pharm J 22(4):343–348. https://doi.org/10.1016/j.jsps.2013.06.001

Odei-Addo F, Shegokar R, Muller RH, Levendal RA, Frost C (2017) Nanoformulation of Leonotis leonurus to improve its bioavailability as a potential antidiabetic drug. 3 Biotech 7(5):344. https://doi.org/10.1007/s13205-017-0986-0

Parveen R, Baboota S, Ali J, Ahuja A, Vasudev SS, Ahmad S (2011) Oil based nanocarrier for improved oral delivery of silymarin: in vitro and in vivo studies. Int J Pharm 413(1–2):245–253. https://doi.org/10.1016/j.ijpharm.2011.04.041

Pathan IB, Setty CM (2011) Enhancement of transdermal delivery of tamoxifen citrate using nanoemulsion vehicle. Int J Pharm Tech Res 3(1):287–297

Pathan IB, Munde SJ, Shelke S, Ambekar W, Setty CM (2019) Curcumin loaded fish scale collagen–HPMC nanogel for wound healing application: ex-vivo and In-vivo evaluation. Int J Polym Mater 68(4):165–174. https://doi.org/10.1080/00914037.2018.1429437

Porter CJ, Trevaskis NL, Charman WN (2007) Lipids and lipid-based formulations: optimizing the oral delivery of lipophilic drugs. Nat Rev Drug Discov 6(3):231–248. https://doi.org/10.1038/nrd2197

Pouton CW, Porter CJ (2008) Formulation of lipid-based delivery systems for oral administration: materials, methods and strategies. Adv Drug Deliv Rev 60(6):625–637. https://doi.org/10.1016/j.addr.2007.10.010

Pratiwi L, Fudholi A, Martien R, Pramono S (2017) Self-nanoemulsifying drug delivery system (Snedds) for topical delivery of mangosteen peels (Garcinia Mangostana L.): formulation design and in vitro studies. J Young Pharm 9(3):341–346. https://doi.org/10.5530/jyp.2017.9.68

Saporito F, Sandri G, Bonferoni MC, Rossi S, Boselli C, Icaro Cornaglia A, Mannucci B, Grisoli P, Vigani B, Ferrari F (2017) Essential oil-loaded lipid nanoparticles for wound healing. Int J Nanomedicine 13:175–186. https://doi.org/10.2147/IJN.S152529

Shakeel F, Shazly GA, Raish M, Ahmad A, Kalam MA, Ali N, Ansari MA, Elosaily GM (2015) Biological investigation of supersaturated self-nanoemulsifying drug delivery system of Piper cubeba essential oil. RSC Adv 5:105206–105217. https://doi.org/10.1039/c5ra22900f

Shakeel F, Alam P, Anwer MK, Alanazi SA, Alsarra IA, Alqarni MH (2019) Wound healing evaluation of self-nanoemulsifying drug delivery system containing Piper cubeba essential oil. 3 Biotech 9(3):82. https://doi.org/10.1007/s13205-019-1630-y

Springer

Sharma G, Beg S, Thanki K, Katare OP, Jain S, Kohli K, Singh B (2015) Systematic development of novel cationic self-nanoemulsifying drug delivery systems of candesartan cilexetil with enhanced biopharmaceutical performance. RSC Adv 5:71500–71513. https://doi.org/10.1039/C5RA11687B

Sidhu GS, Singh AK, Thaloor D, Banaudha KK, Patnaik GK, Srimal RC, Maheshwari RK (1998) Enhancement of wound healing by curcumin in animals. Wound Repair Regen 6(2):167–177

Singh M, Govindarajan R, Nath V, Rawat AKS, Mehrotra S (2006) Antimicrobial, wound healing and antioxidant activity of plagiochasma appendiculatum Lehm. et Lind. J Ethnopharmacol 107(1):67–72. https://doi.org/10.1016/j.jep.2006.02.007

Singh B, Bandopadhyay S, Kapil R, Singh R, Katare O (2009) Self-emulsifying drug delivery systems (SEDDS): formulation development, characterization, and applications. Crit Rev Ther Drug Carrier Syst 26(5):427–521. https://doi.org/10.1615/CritRevTherDrugCarrierSyst.v26.i5.10

Sood S, Jain K, Gowthamarajan K (2014) Optimization of curcumin nanoemulsion for intranasal delivery using design of experiment and its toxicity assessment. Colloids Surf B Biointerfaces 113:330–337. https://doi.org/10.1016/j.colsurfb.2013.09.030

Stejskalova A, Almquist BD (2017) Using biomaterials to rewire the process of wound repair. Biomater Sci 5(8):1421–1434. https://doi.org/10.1039/c7bm00295e

Suntar I, Akkol EK, Keles H, Oktem A, Baser KH, Yesilada E (2011) A novel wound healing ointment: a formulation of *Hypericum perforatum* oil and sage and oregano essential oils based on traditional Turkish knowledge. J Ethnopharmacol 134(1):89–96. https://doi.org/10.1016/j.jep.2010.11.061

Suqumar S, Ghosh V, Nirmala MJ, Mukherjee A, Chandrasekaran N (2014) Ultrasonic emulsification of eucalyptus oil nanoemulsion: antibacterial activity against Staphylococcus aureus and wound healing activity in Wistar rats. Ultrason Sonochem. 21(3):1044–1049. https://doi.org/10.1016/j.ultsonch.2013.10.021

Taha EI, Ak-Suwayeh SA, Tayel MM, Badran MM (2015) Fast ultrafine self-nanoemulsifying drug delivery system for improving in vitro gastric dissolution of poor water soluble drug. Acta Pharm 72(1):171–178

Thacharodi D, Panduranga Rao K (1994) Transdermal absorption of nifedipine from microemulsions of lipophilic skin penetration enhancers. Int J Pharm 111(3):235–240. https://doi.org/10.1016/0378-5173(94)90346-8

Thiruvengadam M, Rajakumar G, Chung IM (2018) Nanotechnology: current uses and future applications in the food industry. 3 Biotech 8(1):74. https://doi.org/10.1007/s13205-018-1104-7

Thomas N, Holm R, Müllertz A, Rades T (2012) *In vitro* and in vivo performance of novel supersaturated self-nanoemulsifying drug delivery systems (super-SNEDDS). J Control Release 160(1):25–32. https://doi.org/10.1016/j.jconrel.2012.02.027

Thomas L, Zakir F, Mirza MA, Anwer MK, Ahmad FJ, Iqbal Z (2017) Development of Curcumin loaded chitosan polymer based nanoemulsion gel: in vitro, ex vivo evaluation and in vivo wound healing studies. Int J Biol Macromol 101:569–579. https://doi.org/10.1016/j.ijbiomac.2017.03.066

Tumen I, Akkol EK, Suntar I, Keles H (2011) Wound repair and anti-inflammatory potential of essential oils from cones of Pinaceae: preclinical experimental research in animal models. J Ethnopharmacol 137(3):1215–1220. https://doi.org/10.1016/j.jep.2011.07.046

Velnar T, Bailey T, Smrkolj V (2009) The wound healing process: an overview of the cellular and molecular mechanisms. J Int Med Res 37:1528–1542. https://doi.org/10.1177/147323000903700531

Villar AM, Naveros BC, Campmany A, Trenchs MA, Rocabert CB, Bellowa LH (2012) Design and optimization of self-nanoemulsifying drug delivery systems (SNEDDS) for enhanced dissolution of gemfibrozil. Int J Pharm 431(1–2):161–175. https://doi.org/10.1016/j.ijpharm.2012.04.001

Wan S, Zhang L, Quan Y, Wei K (2018) Resveratrol-loaded PLGA nanoparticles: enhanced stability, solubility and bioactivity of resveratrol for non-alcoholic fatty liver disease therapy. R Soc Open Sci 5(11):187. https://doi.org/10.1098/rsos.181457

Winter CA, Risley EA, Nuss GW (1963) Anti-Inflammatory and Antipyretic Activities Of Indomethacin, 1-(p-chlorobenzoyl)-5-methoxy-2-methylindole-3-acetic acid. J Pharmacol Exp Ther 141:369–376

Yan YD, Kim JA, Kwak MK, Yoo BK, Yong CS, Choi HG (2011) Enhanced oral bioavailability of curcumin via a solid lipid-based self-emulsifying drug delivery system using a spray-drying technique. Biol Pharm Bull 34(8):1179–1186. https://doi.org/10.1248/bpb.34.1179

Yusufoglu HS, Alqasoumi SI (2011) Anti-inflammatory and wound healing activities of herbal gel containing an antioxidant *Tamarix aphylla* leaf extract. Int J Pharmacol 7(8):829–835. https://doi.org/10.3923/ijp.2011.829.835